arXiv:1505.03956v1 [q-fin.EC] 15 May 2015

From 0D to 1D spatial models using OCMat

D. Graß[1]

[1]ORCOS, Institute of Mathematical Methods in Economics, Vienna University of Technology, A-1040 Vienna, Austria. E-mail: dieter.grass@tuwien.ac.at

May 18, 2015

Abstract

We show that the standard class of optimal control models in OCMat[1]can be used to analyze 1D spatial distributed systems. This approach is an intermediate step on the way to the FEM discretization approach presented in Grass and Uecker [2015]. Therefore, the spatial distributed model is transformed into a standard model by a finite difference discretization. This (high dimensional) standard model is then analyzed using OCMat. As an example we apply this method to the spatial distributed shallow lake model formulated in Brock and Xepapadeas [2008]. The results are then compared with those of the FEM discretization in Grass and Uecker [2015].

Keywords: spatial distributed optimal control model, finite difference discretization, shallow lake model, patterned indifference threshold point

1 Introduction

The analysis of spatial distributed optimal control problems (over an infinite time horizon) become an important issue in economic modeling, see e.g., Brock and Xepapadeas [2008], Brock et al. [2014]. In technical terms this means that the time evolution of the space distributed states are described by parabolic PDEs. In Brock and Xepapadeas [2008] the authors provide a local stability analysis of the equilibria, i.e. the solutions of the elliptic PDEs associated to the derived canonical system. They derive a set of conditions that cause a Turing instability of these equilibria and call the bifurcating patterned equilibria POSS solutions, i.e. Patterned/Heterogeneous Optimal Steady States in contrast to Homogeneous or Flat Optimal Steady States (FOSS).

But, as is shown in Grass and Uecker [2015], a local stability analysis is not sufficient to prove the optimality of heterogeneous equilibria solutions. To answer the question of optimality the objective values of the paths that converge to the different equilibria have to be compared. This analysis also sheds new light on the discussion about indifference threshold and threshold points, cf. Kiseleva and Wagener [2010], Kiseleva [2011]. We therefore introduce a new terminology of defective and non-defective equilibria. This properties distinguishes between optimal equilibria that are stable or unstable.

Since in general the PDEs cannot be solved analytically we have to resort to numerical methods. In Grass and Uecker [2015] we present a numerical procedure relying on a FEM discretization of the derived canonical system combined with a continuation strategy, analogous to the approach in OCMat, cf. Grass [2012]. As an example we used the distributed shallow lake model Eq. (19).

[1]OCMat is a MATLAB package that provides tools for the numerical analysis of (non-distributed) optimal control problems, specifically over an infinite time horizon. It can be downloaded from http://orcos.tuwien.ac.at/research/ocmat_software.

This allowed us to identify parameter regions where non-defective POSS exist, and where defective POSS and the according stable manifolds separates the regions of attractions of FOSS and POSS (threshold points/manifolds). Additionally we were able to show the existence of homogeneous/heterogeneous indifference threshold (Skiba) points and calculated the connecting manifold of indifference threshold points.

In this paper we take an intermediate step to the full FEM approximation of the canonical system, to demonstrate the capabilities of the standard optimal control class of `OCMat`, i.e. infinite time horizon problems, where the time evolution of the states is described by ODEs. To apply the `OCMat` processes for the initialization and file generation directly we discretize the PDEs of the state equations by a finite difference scheme (FD). This yields a number of ODEs that can be handled by `OCMat`. The numerical results of this approach are then compared with the analogous results of Grass and Uecker [2015].

The article is structured in the following way. We start with a discussion and introduction of general terms and shortly present the finite difference discretization in Section 2. In Section 3 we summarize important properties and results of the 0D (non-distributed) shallow lake model, introduced and analyzed in Scheffer [1998], Mäler et al. [2003], Carpenter and Brock. [2004] and Wagener [2003]. In the next Section 4 the 1D spatial distributed shallow lake model is formulated together with its discretized counterpart. The latter model is then numerically analyzed in detail.

2 General Definitions

2.1 Models of spatial dimension 0 (0D model)

$$\max_{u(\cdot)} \int_0^\infty \mathrm{e}^{-\rho t}\, g(x(t), u(t))\mathrm{d}t \tag{1a}$$

$$\text{s.t.} \quad \dot{x}(t) = f(x(t), u(t)) \tag{1b}$$

$$x(0) = x_0 \in \mathbb{R}^n. \tag{1c}$$

with $f \in C^2(\mathbb{R}^n \times \mathbb{R}^m, \mathbb{R}^n)$, $g \in C^2(\mathbb{R}^n \times \mathbb{R}^m, \mathbb{R})$.

Let $(x^*(\cdot), u^*(\cdot))$ be an optimal solution of Eq. (1). Then there exists $\lambda(\cdot)$ such that $(x^*(\cdot), u^*(\cdot), \lambda(\cdot))$ is a solution of the canonical system

$$\dot{x}(t) = f(x^*(t), u(t)) \tag{2a}$$

$$\dot{\lambda}(t) = \rho\lambda(t) - \mathcal{H}(x^*(t), u^*(t), \lambda(t), \lambda_0) \tag{2b}$$

$$x^*(0) = x_0 \tag{2c}$$

with

$$u^*(t) = \operatorname*{argmax}_u \mathcal{H}(x^*(t), u, \lambda(t), \lambda_0) \tag{2d}$$

and

$$\mathcal{H}(x, u, \lambda, \lambda_0) := \lambda_0 g(x, u) + \lambda^\top f(x, u), \tag{2e}$$

To ease the notation we make the following assumptions

Assumption 2.1. *Problem Eq. (1) is normal, i.e., $\lambda_0 = 1$. Therefore, we omit the argument λ_0.*

Assumption 2.2. *Let $(x^*(\cdot), u^*(\cdot))$ be an optimal solution and $\lambda(\cdot)$ the according costate. Then, there exists an explicit function*

$$u^\circ(x, \lambda) \in C^2\left(\mathbb{R}^n \times \mathbb{R}^n, \mathbb{R}^m\right),$$

such that for every t

$$\mathcal{H}(x^*(t), u^\circ(x^*(t), \lambda(t)), \lambda(t)) = \max_u \mathcal{H}(x^*(t), u, \lambda(t)).$$

Then an optimal solution $(x^*(\cdot), u^*(\cdot))$ can be found among the solutions satisfying

$$\dot{x}(t) = \bar{f}(x(t), \lambda(t)) \tag{3a}$$
$$\dot{\lambda}(t) = \rho\lambda(t) - \bar{\mathcal{H}}_x(x(t), \lambda(t)) \tag{3b}$$
$$x(0) = x_0. \tag{3c}$$

with

$$\bar{f}(x(t), \lambda(t)) := f(x(t), u^\circ(x(t), \lambda(t)))$$

and

$$\bar{\mathcal{H}}(x(t), \lambda(t)) := \mathcal{H}(x(t), u^\circ(x(t), \lambda(t)), \lambda(t), 1). \tag{3d}$$

Subsequently we will omit the bar sign.

Definition 2.1 (OSS)**.** *Let $(x^*(\cdot), u^*(\cdot))$ with $x^*(\cdot) \equiv \hat{x} \in \mathbb{R}^n$ and $u^*(\cdot) \equiv \hat{u} \in \mathbb{R}^m$ be an optimal solution of problem (1) with $x(0) = \hat{x}$. Then $(\hat{x}, \hat{u})$ is called an* optimal equilibrium *and denoted as OSS.*

Let $(\hat{x}, \hat{\lambda}) \in \mathbb{R}^{2n}$ be an equilibrium of the canonical system Eq. (3). Then $(\hat{x}, \hat{\lambda}) \in \mathbb{R}^{2n}$ is denoted as CSS and

$$J(\hat{x}, \hat{\lambda}) := \left(\begin{array}{cc} \dfrac{\mathrm{d}f(x,\lambda)}{\mathrm{d}x} & \dfrac{\mathrm{d}f(x,\lambda)}{\mathrm{d}\lambda} \\ -\dfrac{\mathrm{d}\mathcal{H}^\circ(x,\lambda)}{\mathrm{d}x} & r - \dfrac{\mathrm{d}\mathcal{H}^\circ(x,\lambda)}{\mathrm{d}\lambda} \end{array} \right) \Bigg|_{(\hat{x},\hat{\lambda})} \tag{4}$$

is the according *Jacobian matrix*, and if there is no ambiguity we simply write $\hat{J}$. The eigenspaces corresponding to $J(\hat{x}, \hat{\lambda})$ are denoted as

$$\mathrm{E}^s(\hat{x}, \hat{\lambda}) := \{\xi \in \mathbb{C} : \ J(\hat{x}, \hat{\lambda})v = \xi v \text{ with } \operatorname{Re}\xi < 0\}, \ n_s := \dim \mathrm{E}^s(\hat{x}, \hat{\lambda}) \tag{5a}$$
$$\mathrm{E}^u(\hat{x}, \hat{\lambda}) := \{\xi \in \mathbb{C} : \ J(\hat{x}, \hat{\lambda})v = \xi v \text{ with } \operatorname{Re}\xi > 0\}, \ n_u := \dim \mathrm{E}^u(\hat{x}, \hat{\lambda}) \tag{5b}$$
$$\mathrm{E}^c(\hat{x}, \hat{\lambda}) := \{\xi \in \mathbb{C} : \ J(\hat{x}, \hat{\lambda})v = 0\}, \ n_c := \dim \mathrm{E}^c(\hat{x}, \hat{\lambda}). \tag{5c}$$

Definition 2.2 (Saddle Point Property)**.** *Let $(\hat{x}, \hat{\lambda}) \in \mathbb{R}^{2n}$ be an equilibrium of Eq. (3). If*

$$\dim \mathrm{E}^s(\hat{x}, \hat{\lambda}) = n \tag{6}$$

then it is said, that the equilibrium satisfies the saddle point property (SPP)*. The equilibrium $(\hat{x}, \hat{\lambda})$ is denoted as CSS^0. Otherwise it is denoted as CSS$^-$. The number*

$$\mathrm{d}(\hat{x}, \hat{\lambda}) := n_s - n_u - n_c \tag{7}$$

is called the defect *of $(\hat{x}, \hat{\lambda})$. An equilibrium with defect $\mathrm{d}(\hat{x}, \hat{\lambda}) < 0$ is called* defective*, otherwise it is called* non-defective*. If $(\hat{x}, \hat{\lambda})$ is defective and the according $(\hat{x}, u^\circ(\hat{x}, \hat{\lambda}))$ is OSS, then $(\hat{x}, u^\circ(\hat{x}, \hat{\lambda}))$ is called* defective *otherwise it is called* non-defective*.*

Proposition 2.1. *Let $(\hat{x}, \hat{\lambda}) \in \mathbb{R}^{2n}$ be an equilibrium of Eq. (3) and $\rho > 0$. Then $(\hat{x}, \hat{\lambda})$ satisfies the saddle point property iff every eigenvalue ξ of the according Jacobian $J(\hat{x}, \hat{\lambda})$ satisfies*

$$|\operatorname{Re}\xi - \frac{\rho}{2}| > \frac{\rho}{2} \tag{8}$$

Proof. In Grass et al. [2008] it is proved that there exist n (not necessarily distinct) complex numbers $\bar{\xi} \in \mathbb{C}$ with $\operatorname{Re}\bar{\xi} \geq 0$ such that any eigenvalue ξ of the according Jacobian, satisfies

$$\xi = \frac{\rho}{2} + \bar{\xi} \quad \text{or} \quad \xi = \frac{\rho}{2} - \bar{\xi}.$$

This symmetry together with SPP yields

$$|\operatorname{Re}\xi - \frac{\rho}{2}| = \operatorname{Re}\bar{\xi} > \frac{\rho}{2}$$

and the last inequality is identical to

$$\operatorname{Re}\bar{\xi} > \frac{\rho}{2} \quad \text{iff} \quad \operatorname{Re}\xi < 0.$$

Therefore, n eigenvalues have a negative real part finishing the proof. □

Remark 2.1. *Proposition 2.1 allows us to formulate the SPP by the equivalent Eq. (8). A definition of SPP claiming Eq. (8) has the advantage that it also can be applied to equilibria of distributed systems. Where a definition relying on the dimension of the stable manifold fails.*

2.2 Models of spatial dimension 1 (1D model)

We assume that the spatially distributed model is derived by the introduction of a diffusion term, whereas the functions f and g are the same as for model (1). This yields

$$\begin{aligned}
&\max_{u(\cdot,\cdot)} \int_0^\infty \int_{-L}^{L} \mathrm{e}^{-\rho t}\, g(x(z,t),u(z,t))\mathrm{d}z\mathrm{d}t \\
\text{s.t.}\quad &\frac{\partial}{\partial t}x(z,t) = f(x(z,t),u(z,t)) + D\frac{\partial^2 x(z,t)}{\partial z^2} \\
&\left.\frac{\partial x(z,t)}{\partial z}\right|_{\pm L} = 0 \\
&x(z,0) = x_0(z), \quad z \in [-L,L].
\end{aligned}$$

Or transforming $[-L,L]$ into $[0,1]$ yields

$$\max_{u(\cdot,\cdot)} \int_0^\infty \int_0^1 \mathrm{e}^{-\rho t}\, g(x(z,t),u(z,t))\mathrm{d}z\mathrm{d}t \tag{9a}$$

$$\text{s.t.}\quad \frac{\partial}{\partial t}x(z,t) = f(x(z,t),u(z,t)) + \frac{D}{(2L)^2}\frac{\partial^2 x(z,t)}{\partial z^2} \tag{9b}$$

$$\left.\frac{\partial x(z,t)}{\partial z}\right|_{0,1} = 0 \tag{9c}$$

$$x(z,0) = x_0(z), \quad z \in [0,1]. \tag{9d}$$

Applying Pontryagin's Maximum Principle for PDEs, see e.g., Tröltzsch [2009], we can derive, analogous to Eq. (3), the canonical system for (9) as

$$\frac{\partial}{\partial t}x(z,t) = f(x(z,t),\lambda(z,t)) + D\frac{\partial^2 x(z,t)}{\partial x^2} \tag{10a}$$

$$\frac{\partial}{\partial t}\lambda(z,t) = \rho\lambda(z,t) - \frac{\partial \mathcal{H}(x(z,t),\lambda(z,t))}{\partial x} - D\frac{\partial^2 \lambda(z,t)}{\partial x^2} \tag{10b}$$

$$\partial_n x(z,t)|_{0,1} = 0 \tag{10c}$$

$$\partial_n \lambda(z,t)|_{0,1} = 0 \tag{10d}$$

$$x(z,0) = x_0(z), \quad z \in [0,1]. \tag{10e}$$

For the numerical analysis we can than e.g. use a finite element method (FEM) for the discretization of Eq. (10). For the distributed shallow lake model (cf. Section 4) this has been carried out in Grass

and Uecker [2015]. In this article we want to demonstrate the capabilities of `OCMat` and transform it into a high dimensional 0D model.

For the FDM discretization we use an equidistant grid of length h with $Nh = 1$ and $N \in \mathbb{N}$.

$$\left.\frac{\mathrm{d}}{\mathrm{d}z}x(z)\right|_{z_i} \approx \frac{x(z_i+h) - x(z_i-h)}{2h} \tag{11a}$$

$$\left.\frac{\mathrm{d}^2}{\mathrm{d}z^2}x(z)\right|_{z_i} \approx \frac{x(z_i-h) - 2x(z_i) + x(z_i+h)}{h^2} \tag{11b}$$

$$\int_0^1 g(z)\mathrm{d}x \approx h\left(\sum_{i=1}^{N-1} g(z_i) + \frac{g(z_0)+g(z_N)}{2}\right) \tag{11c}$$

Thus, model (9) is approximated by

$$\max_{u_0(\cdot),\dots,u_N(\cdot)} \frac{1}{N}\left\{\int_0^\infty \mathrm{e}^{-\rho t}\left(\sum_{i=1}^{N-1} g(x_i(t),u_i(t)) + \frac{g(x_0(t),u_0(t)) + g(x_N(t),u_N(t))}{2}\right)\mathrm{d}t\right\} \tag{12a}$$

$$\text{s.t.}\quad \dot{x}_i(t) = f(x_i(t),u_i(t)) + \frac{DN^2}{(2L)^2}\left(x_{i-1}(t) - 2x_i(t) + x_{i+1}(t)\right) \tag{12b}$$

$$x_1(t) - x_{-1}(t) = x_{N+1}(t) - x_{N-1}(t) = 0, \quad t \geq 0 \tag{12c}$$

$$x_i(0) = x_{i,0}. \tag{12d}$$

with

$$z_i = \frac{i}{N}, \quad i = 0,\dots,N$$
$$x_i(t) := x(z_i,t), \quad u_i(t) := u(z_i,t)$$
$$x_i := x(z_i,\cdot), \quad u_i := u(z_i,\cdot)$$

Note that we do not consider the problem under which conditions model (12) approximates (9). We rather take, in the specific case of the spatial shallow lake model, model (12) for granted to see if `OCMat` can handle such a problem and compare the results with those from Grass and Uecker [2015].

The canonical system for model (12) becomes

$$\dot{x}_i(t) = f(x_i(t),\lambda_i(t)) + \mathcal{D}_i^{(x)}(t) \tag{13a}$$

$$\dot{\lambda}_i(t) = \rho\lambda_i(t) - \mathcal{H}_x(x_i(t),\lambda_i(t)) - \mathcal{D}_i^{(\lambda)}(t) \tag{13b}$$

$$x_i(0) = x_{i,0}. \tag{13c}$$

and

$$u_i^\circ = u_i(x_i,\lambda_i)$$
$$\tilde{D} := \frac{DN^2}{(2L)^2}$$
$$\mathcal{D}_i^{(x)} := \begin{cases} 2\tilde{D}(x_1 - x_0) & i = 0 \\ \tilde{D}(x_{i-1} - 2x_i + x_{i+1}) & i = 1,\dots,N-1 \\ 2\tilde{D}(x_{N-1} - x_N) & i = N \end{cases}$$
$$\mathcal{D}_i^{(\lambda)} := \begin{cases} \tilde{D}(\lambda_1 - 2\lambda_0) & i = 0 \\ \tilde{D}(2\lambda_0 - 2\lambda_1 + \lambda_2) & i = 1 \\ \tilde{D}(\lambda_{i-1} - 2\lambda_i + \lambda_{i+1}) & i = 2,\dots,N-2 \\ \tilde{D}(\lambda_{N-2} - 2\lambda_{N-1} + 2\lambda_N) & i = N-1 \\ \tilde{D}(\lambda_{N-1} - 2\lambda_N & i = N) \end{cases}$$

To abbreviate notation we introduce

$$x^d := (x_0^\top, \dots, x_N^\top)^\top \in \mathbb{R}^{n(N+1)}$$
$$\lambda^d := (\lambda_0^\top, \dots, \lambda_N^\top)^\top \in \mathbb{R}^{n(N+1)}$$
$$u^d := (u_0^\top, \dots, u_N^\top)^\top \in \mathbb{R}^{m(N+1)}.$$

Definition 2.3 (FOSS and POSS)**.** *Let* $(x^{d,*}(\cdot), u^{d,*}(\cdot))$ *with* $x^{d,*}(\cdot) \equiv \hat{x}^d \in \mathbb{R}^{n(N+1)}$ *and* $u^{d,*}(\cdot) \equiv \hat{u}^d \in \mathbb{R}^{m(N+1)}$ *be an optimal solution of problem* (1) *with* $x^d(0) = \hat{x}^d$ *. If*

$$\hat{x}_0 = \hat{x}_1 = \cdots = \hat{x}_N = \hat{x} \in \mathbb{R}^n$$

then $(\hat{x}^d, \hat{u}^d)$ *is called a* flat (homogeneous) optimal steady state (FOSS)*, otherwise it is called an* patterned (heterogeneous) optimal steady state (POSS)*.*

Definition 2.4 (FCSS and PCSS)**.** *Let* $(\hat{x}^d, \hat{\lambda}^d) \in \mathbb{R}^{2n(N+1)}$ *be an equilibrium of the canonical system Eq.* (13)*. Then* $(\hat{x}^d, \hat{\lambda}^d)$ *is called a* flat (homogeneous) steady state (FCSS) *iff*

$$\hat{x}_0 = \hat{x}_1 = \cdots = \hat{x}_N = \hat{x} \tag{14}$$

otherwise it is called a patterned (heterogeneous) steady state (PCSS)*. If a FCSS (PCSS) satisfies SPP it is denoted as FCSS*^{0} *(PCSS*^{0}*) otherwise it is denoted as FCSS*$^-$ *(PCSS*$^-$*).*

Definition 2.5 (State-Costate space)**.** *Let* $(x^d(\cdot), \lambda^d(\cdot))$ *be a solution of the canonical system Eq.* (13)*. Then the representation* $(\|x^d\|(\cdot), \|\lambda^d\|(\cdot))$ *with*

$$\|y_j^d\|(t) := \frac{1}{N}\left(\sum_{i=1}^{N-1}\|y_j^i(t)\| + \frac{\|y_j^0(t)\| + \|y_j^N(t)\|}{2}\right), \quad y = x, \text{ or } y = \lambda, \ j = 1, \dots, n. \tag{15}$$

is called a solution path in the state-costate space*.*

Remark 2.2. *In Brock and Xepapadeas [2008] FOSS (POSS) were introduced as* flat (patterned) optimal equilibria *of the canonical system satisfying SPP. We enhanced this terminology for two reasons*

1. *For better clearness we decided to make a further distinction between the canonical and optimal system.*
2. *There exist optimal equilibria that do not satisfy SPP, cf. Section 4.4.1.*

3 The shallow lake model without spatial diffusion

A well known version of the shallow lake model, see e.g. Wagener [2003], can be formulated as

$$\max_{u(\cdot)} \int_0^\infty \mathrm{e}^{-\rho t}\left(\ln(u(t)) - cP(t)^2\right)\mathrm{d}t \tag{16a}$$
$$\text{s.t.} \quad \dot{P}(t) = u(t) - bP(t) + \frac{P(t)^2}{1 + P(t)^2} \tag{16b}$$
$$P(0) = P_0 > 0. \tag{16c}$$

We sometimes refer to model (16) as *0D shallow lake model*.

By Pontryagin's Maximum Principle we find the canonical system

$$\dot{P}(t) = u^{\circ}(t) - bP(t) + \frac{P(t)^2}{1+P(t)^2} \tag{17a}$$

$$\dot{\lambda}(t) = 2cP(t) + \lambda(t)\left(\rho + b - \frac{2P(t)}{(1+P(t)^2)^2}\right) \tag{17b}$$

$$P(0) = P_0 \tag{17c}$$

with

$$u^{\circ}(t) = -\frac{1}{\lambda(t)}. \tag{17d}$$

Let $(P^*(\cdot), u^*(\cdot))$ be the optimal solution of Eq. (16); then $P^*(\cdot)$ is the unique solution of the IVP

$$\dot{P}(t) = u^*(t) - bP(t) + \frac{P(t)^2}{1+P(t)^2} \tag{18a}$$

$$P(0) = P_0. \tag{18b}$$

The ODE (18a) is called the *optimal system* for $u^*(t)$. In Wagener [2003] it is proved that every optimal solution $(P^*(\cdot), u^*(\cdot))$ for arbitrary $P_0 > 0$ converges to an equilibrium $(\hat{P}, \hat{u})$ of the optimal system with $\hat{u} > 0$, usually depending on P_0.

A detailed bifurcation analysis in the parameter space (b, c), see, e.g., Wagener [2003], reveals the existence of regions in the parameter space where the optimal system consists of

- One globally stable optimal equilibrium $(\hat{P}, \hat{u})$.
- Two locally stable equilibria $(\hat{P}_o, \hat{u}_o)$ and $(\hat{P}_e, \hat{u}_e)$. These are separated by one of the following state values
  - The state value $\hat{P}_u$ of an unstable optimal equilibrium $(\hat{P}_u, \hat{u}_u)$.
  - An indifference threshold point P_I also called Skiba point.

Thus, we can give a full classification of the optimal solutions. In the case that three optimal equilibria exist we choose $\hat{P}_o$ and $\hat{P}_e$ such that $\hat{P}_o < \hat{P}_u < \hat{P}_e$. There are intermediate cases (bifurcation cases) where equality holds that are not specifically mentioned. We also refer to $\hat{P}_e$ as the *eutrophic* and to $\hat{P}_o$ as the *oligotrophic* equilibrium.

Global stable: For any initial state $P_0 > 0$ there exists a unique solution $(P^*(\cdot), u^*(\cdot))$ that converges to $(\hat{P}, \hat{u})$, which is independent of P_0. See Fig. 2c.

Local stable I: For any initial state $0 < P_0 < \hat{P}_u$ there exists a unique solution $(P^*(\cdot), u^*(\cdot))$ that converges to $(\hat{P}_o, \hat{u}_1)$, which is independent of P_0. For $P_0 > \hat{P}_u$ there exists a unique solution $(P^*(\cdot), u^*(\cdot))$ that converges to $(\hat{P}_e, \hat{u}_2)$, which is independent of P_0. For $P_0 = \hat{P}_u$ the optimal solution is $(P^*(\cdot), u^*(\cdot)) \equiv (\hat{P}_u, \hat{u}_u)$. See Fig. 3c. $\hat{P}_u$ is called a *threshold point*.

Local stable II: The first two statements of the previous case remain true, replacing $\hat{P}_u$ by P_I. For $P_0 = P_I$ there exist two optimal solutions $(P_i^*(\cdot), u_i^*(\cdot))$, $i = 1, 2$ that converge to $(\hat{P}_o, \hat{u}_1)$ and $(\hat{P}_e, \hat{u}_2)$ with $\hat{P}_o < P_I < \hat{P}_e$. See Fig. 4c. P_I is called an *indifference threshold point* or *Skiba point*.

From the perspective of optimal control theory the last two cases are of specific interest. The first case is often referred to as *history dependence*, i.e., the optimal solution depends on its initial starting point. In the second case we additionally observe the non-uniqueness of the optimal solution, i.e., *indifference*. For a detailed discussion and description of the underlying bifurcations we refer to Kiseleva and Wagener [2010], Kiseleva [2011].

The parameter values for these two prototypical cases are specified in Table 1. In the first case we find an indifference threshold point and in the second case a threshold point.

Model (16)				Model (19) specific		
Scenario	ρ	c	b	D	L	N
I	0.03	0.5	0.65^*	0.5	$2\pi/0.44$	50
II	0.3	3.5^*	0.55	0.5	$2\pi/0.44$	50

Table 1: The parameter values for the two considered scenarios for the 0D and 1D model. The values with the superscript * denote the free parameter.

Bifurcation-analysis Anyhow, this classification is the result of an intensive numerical analysis of the canonical system Eq. (17). This analysis covers a bifurcation analysis of its equilibria (see Fig. 1) and the calculation of the related stable paths and their objective value. The numerical computation is necessary since the local properties of an equilibrium $(\hat{P}, \hat{\lambda})$ of Eq. (17) let us not deduce that the corresponding equilibrium $(\hat{P}, \hat{u})$ with $\hat{u} = 1/\hat{\lambda}$ is an optimal equilibrium of the optimal system Eq. (18a). This is specifically true in the case that multiple equilibria of the canonical system exist. Therefore, there is no one-to-one correspondence between the bifurcations of the optimal and canonical system.

Unique optimal equilibrium The importance of a numerical analysis of the stable paths comes specifically clear in scenario I with $b = 0.75$. In Fig. 2 we see that there exist three equilibria in the canonical system (two saddles and one unstable focus), whereas the optimal system only consists of one globally stable equilibrium.

Indifference threshold point For $b = 0.65$ the number and properties of the equilibria of the canonical system remain the same, but the optimal system consists of two locally stable equilibria separated by an indifference threshold point P_I, cf. Fig. 3. Thus, a local stability analysis of the equilibria has to be supported by the global analysis the according stable manifolds. Even if the first task can be realized analytically, the stable paths can only be calculated analytically in very rare cases. Usually and specifically in our case we have to resort to numerical methods to solve the latter task.

Indifference point For scenario II with $c = 3.5$ the canonical system exhibits two saddles and one unstable node (cf. Fig. 4a). Calculating the stable paths and comparing the objective values we find that the unstable equilibrium is a threshold point (cf. Fig. 4b). This unstable equilibrium separates the regions of attraction for the two locally stable equilibria corresponding to the two saddles(cf. Fig. 4c). The second case with $c = 3.0825$ yields qualitatively the same result and is not depicted.

4 The shallow lake model with spatial diffusion

An extension of the shallow lake model (16) to the class of spatially distributed models, proposed in Brock and Xepapadeas [2008], is given by

$$\max_{u(\cdot,\cdot)} \int_0^\infty \mathrm{e}^{-\rho t} \int_\Omega \ln(u(x,t)) - cP(x,t)\mathrm{d}x\,\mathrm{d}t \tag{19a}$$

$$\text{s.t.} \quad \frac{\partial}{\partial t}P(x,t) = u(x,t) - bP(x,t) + \frac{P(x,t)^2}{1+P(x,t)^2} + D\frac{\partial^2}{\partial x^2}P(x,t) \tag{19b}$$

$$\partial_n P(x,t)|_{\partial\Omega} = 0 \tag{19c}$$

$$P(x,t)|_{t=0} = P_0(x), \quad x \in \Omega = [-L, L] \subset \mathbb{R}. \tag{19d}$$

Contrary to Brock and Xepapadeas [2008] we formulated the problem for Neumann conditions Eq. (19c), the so called zero flux boundary condition, instead of the periodic boundary conditions. From an interpretational point of view we assume the lakes to be located consecutively in a row and there is

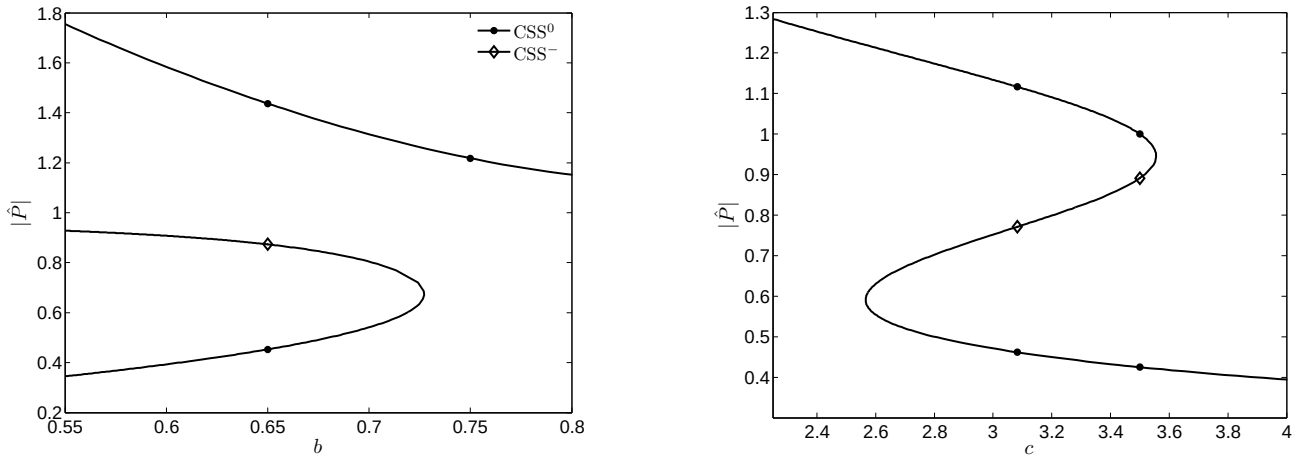

(a) Equilibria bifurcation diagram

(b) Equilibria bifurcation diagram

Figure 1: The • denote equilibria satisfying the SPP and ⋄ denote equilibria not satisfying SPP. The figures in the first row show the bifurcation parameter versus the (absolute) state value. In the second row the norm of the equilibrium is plotted versus the bifurcation parameter. Panel (a) ($\rho = 0.03, c = 0.5$ and varying b) show the existence of two separated branches of equilibria. In the interval $[0, 0.727]$ there exist three equilibria. Panel (b) ($\rho = 0.3, b = 0.55$ and varying c) shows the existence of one branch of equilibria. In the interval $[2.566, 3.556]$ there exist three equilibria.

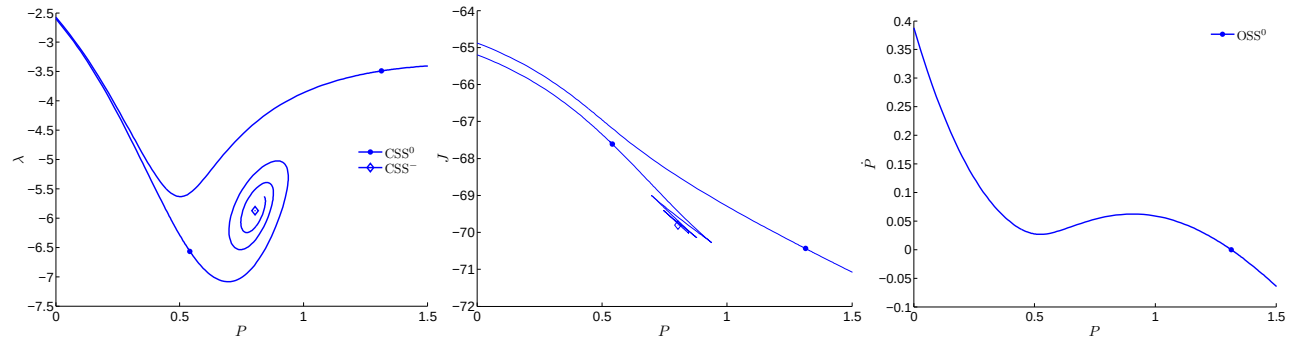

(a) State-Costate

(b) State-Objectivevalue

(c) Optimal System

Figure 2: For $\rho = 0.03$, $c = 0.5$ and $b = 0.75$ there exist three equilibria in the canonical system (a). The optimal system (c) only consist of one globally optimal equilibrium. In panel (a) the • denote saddles of the canonical system, the ⋄ an unstable focus. In panel (c) the • denotes the globally stable equilibrium.

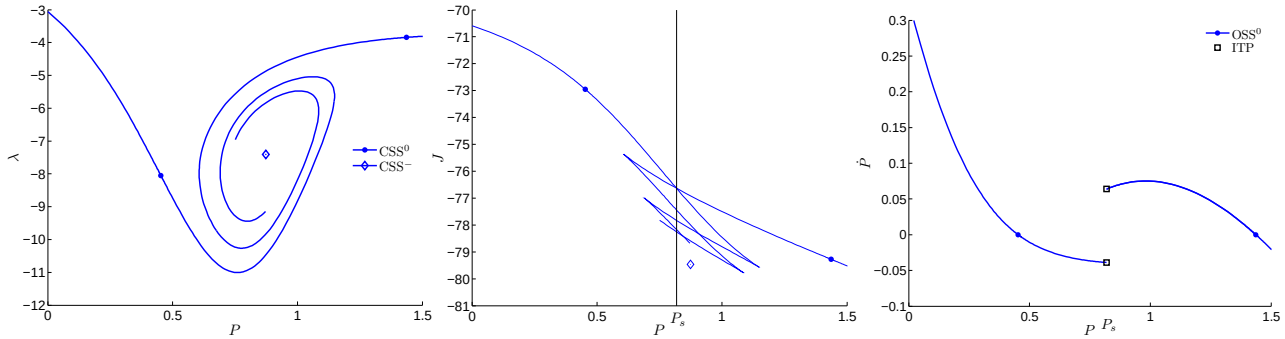

(a) State-Costate (b) State-Objectivevalue (c) Optimal System

Figure 3: For $\rho = 0.03$, $c = 0.5$ and $b = 0.65$ there exist three equilibria in the canonical system (a). The optimal system (c) consists of two locally optimal equilibria. The basins of attraction are separated by an indifference threshold point (Skiba point) P_I, with a discontinuous dynamics at P_I. In panel (a) the • denote saddles of the canonical system, the ⋄ an unstable focus. In panel (c) the • denote the locally stable equilibria.

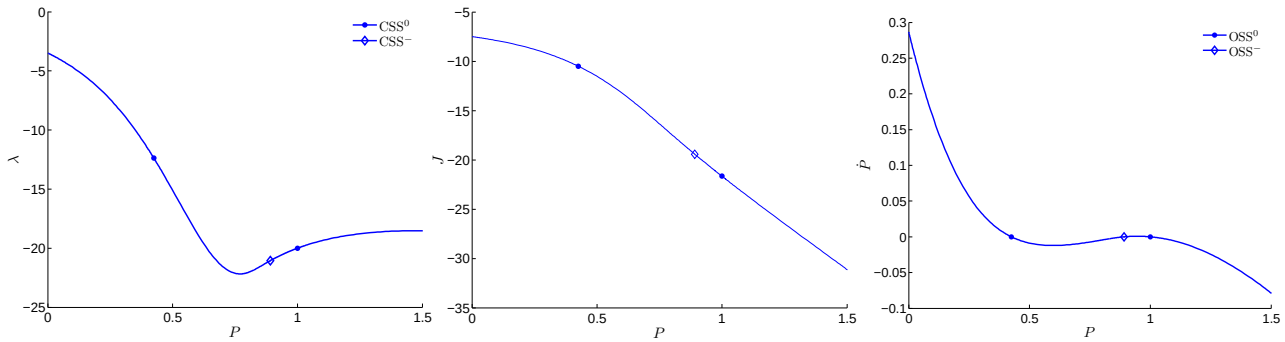

(a) State-Costate (b) State-Objectivevalue (c) Optimal System

Figure 4: For $\rho = 0.3$, $c = 3.5$ and $b = 0.55$ there exist three equilibria in the canonical system (a). The optimal system (c) consists of two locally optimal equilibria. The basins of attraction are separated by the optimal unstable equilibrium $\hat{P}_u$. In panel (a) • denote saddles of the canonical system, ⋄ an unstable node. In panel (c) • denote the locally stable optimal equilibria and ⋄ denotes the optimal unstable node.

no flow out of lake. Periodic boundary conditions refer to a ring of lakes. Brock and Xepapadeas argue that they use periodic boundary conditions to exclude effects induced by the conditions at the end points. Anyhow, since this point does not touch our argument that it is necessary to analyze the global behavior of the optimally controlled system, we changed the model formulation in this respect.

Using the (FDM) discretization proposed in Section 2.2 we find

$$\max_{u_0(\cdot),\ldots,u_N(\cdot)} \left\{ \int_0^\infty \mathrm{e}^{-rt}\, G(P_0(t),\ldots,P_N(t),u_0(t),\ldots,u_N(t))\ \mathrm{d}t \right\} \tag{20a}$$

$$\text{s.t. } \dot{P}_i(t) = u_i(t) - bP_i(t) + \frac{P_i(t)^2}{1+P_i(t)^2} + \tilde{D}\left(P_{i-1}(t) - 2P_i(t) + P_{i+1}(t)\right) \tag{20b}$$

$$P_1(t) - P_{-1}(t) = P_{N+1}(t) - P_{N-1}(t) = 0, \quad t \geq 0 \tag{20c}$$

$$P_i(0) = P_{i,0} > 0 \tag{20d}$$

with

$$x_i = \frac{i}{N}, \quad i = 0,\ldots,N, \quad \tilde{D} := D\left(\frac{N}{2L}\right)^2$$

$$P_i(t) := P(x_i,t), \quad u_i(t) := u(x_i,t)$$

$$P_i := P(x_i,\cdot), \quad u_i := u(x_i,\cdot)$$

$$G(P_0,\ldots,P_N,u_0,\ldots,u_N) := \frac{1}{N}\sum_{i=1}^{N-1} g(P_i,u_i) + \frac{g(P_0,u_0)+g(P_N,u_N)}{2}$$

$$g(P_i,u_i) := \ln(u_i) - cP_i^2$$

Applying Pontryagin's Maximum Principle on Eqs. (11) yields the canonical system

$$\dot{P}_i(t) = u_i^\circ(t) - bP_i(t) + \frac{P_i(t)^2}{1+P_i(t)^2} + \mathcal{D}_i^{(P)}(t) \tag{21a}$$

$$\dot{\lambda}_i(t) = c_i P_i(t) + \lambda_i(t)\left(\rho + b - \frac{2P_i(t)}{(1+P_i(t)^2)^2}\right) - \mathcal{D}_i^{(\lambda)}(t) \tag{21b}$$

$$P_i(0) = P_{i,0} > 0, \quad i = 0,\ldots,N \tag{21c}$$

$$u_i^\circ(t) = \begin{cases} -\dfrac{1}{2\lambda_i(t)} & i = 0, N \\ -\dfrac{1}{\lambda_i(t)} & i = 1,\ldots,N-1 \end{cases} \tag{21d}$$

$$c_i := \begin{cases} c & i = 0, N \\ 2c & i = 1,\ldots,N-1 \end{cases}$$

$$\mathcal{D}_i^{(P)}(t) := \begin{cases} 2\tilde{D}(P_1(t) - P_0(t)) & i = 0 \\ \tilde{D}(P_{i-1}(t) - 2P_i(t) + P_{i+1}(t)) & i = 1,\ldots,N-1 \\ 2\tilde{D}(P_{N-1}(t) - P_N(t)) & i = N \end{cases}$$

$$\mathcal{D}_i^{(\lambda)}(t) := \begin{cases} \tilde{D}(\lambda_1(t) - 2\lambda_0(t)) & i = 0 \\ \tilde{D}(2\lambda_0(t) - 2\lambda_1(t) + \lambda_2(t)) & i = 1 \\ \tilde{D}(\lambda_{i-1}(t) - 2\lambda_i(t) + \lambda_{i+1}(t)) & i = 2,\ldots,N-2 \\ \tilde{D}(\lambda_{N-2}(t) - 2\lambda_{N-1}(t) + 2\lambda_N(t)) & i = N-1 \\ \tilde{D}(\lambda_{N-1}(t) - 2\lambda_N(t)) & i = N \end{cases}$$

In Appendix B the details for an implementation of the model (20) in `OCMat` are explained.

4.1 Equilibria of the canonical/optimal system

There is an intimate relation between the CSS of the canonical system Eq. (17) and FCSS of the canonical system Eq. (21)

Corollary 4.1. *Let* $(\hat{P}^d, \hat{u}^d) \in \mathbb{R}^{2N+2}$ *be FOSS then* $(\hat{P}_0^d, 1/(2u_0))$ *is an equilibrium of the canonical system Eq.* (17)*.*

Corollary 4.2. *Let* $(\hat{P}, \hat{\lambda})$ *be an equilibrium of the canonical system Eq.* (17)*. Then* $\hat{P}^d := (\hat{P}, \dots, \hat{P})$ *and* $\hat{\lambda}^d := (2\hat{\lambda}, \hat{\lambda}, \dots, \hat{\lambda}, 2\hat{\lambda})$ *is a FCSS.*

Corollary 4.3. *Let* $(\hat{P}, \hat{\lambda})$ *be a saddle of the canonical system Eq.* (17)*. Then for* $\tilde{D}$ *small enough* $(\hat{P}^d, \hat{\lambda}^d) \in \mathbb{R}^{2N+2}$ *defined in Corollary 4.2 is FCSS*^{0}*.*

PCSS can in general not be calculated analytically therefore we have to resort to numerical methods. Using Corollary 4.2 we can start a bifurcation analysis of Eq. (21) with an equilibrium of Eq. (17). The PCSS emerge from branching points of the bifurcation curve. In Grass and Uecker [2015] the according bifurcation analysis is done using `pde2path`, a MATLAB package for the bifurcation analysis of elliptic PDEs, see Uecker et al. [2014] and Dohnal et al. [2014]. Since the actual model (16) is a 0D optimal control model with a finite number of states $(N + 1)$ the bifurcation analysis of Eq. (21) is done using a modified version of `CL_MATCONT`[2].

We analyzed the two different scenarios specified in Table 1.

First Scenario The according bifurcation analysis with respect to b is depicted in Fig. 5a. The black curves represent the bifurcation curves of the FCSS. These curves exhibit the same shape as the corresponding bifurcation curves for the 0D model in Fig. 1a. For the lower branch we additionally find four branching points ∘, where the branches of the PCSS emanate (red, green, magenta and cyan). Along the bifurcation curves of the PCSS we find additional branching points and calculated the according bifurcation curves (brown, dark green and orange). Thus, for $b = 0.65$ we find in total two FCSS^0 (correspondig to the oligotrophic and eutrophic equilibrium in the 0D model), one FCSS$^-$, thirteen PCSS$^-$ and one PCSS^0. In fact the brown and dark green branch consists of two distinct bifurcation curves with equilibria that are spatially symmetric.

Second Scenario The according bifurcation analysis with respect to c is depicted in Fig. 5b. The black bifurcation curve of the FCSS consists of one branch, exhibiting two fold bifurcations and six branching points ∘. These six branching points are connected by three bifurcation curves of the PCSS (red, magenta and green). The red and green curve consist of two spatially symmetric branches. From the magenta PCSS bifurcation curve two further PCSS branches emanate (brown and orange).

In Section 4.4 we consider two specific cases for $c = 3.5$ and $c = 3.0825$. In the first case there exist two FCSS^0 (correspondig to the oligotrophic and eutrophic equilibrium in the 0D model), one FCSS$^-$, ten PCSS$^-$ and two PCSS^0. In the latter case there exist two FCSS^0, one FCSS$^-$ and four PCSS$^-$.

4.2 First scenario optimal solutions exemplified on two cases

Most of the results for the specific cases $b = 0.75$ and $b = 0.65$ have already been discussed in Grass and Uecker [2015]. Therefore we only give a brief summary and concentrate on some aspects that were easier to get using `OCMat`.

For $b = 0.75$ there exists a single FOSS, structurally reproducing the result of the according 0D model.

For $b = 0.65$ the main results are

[2]This modified version is available from the author.

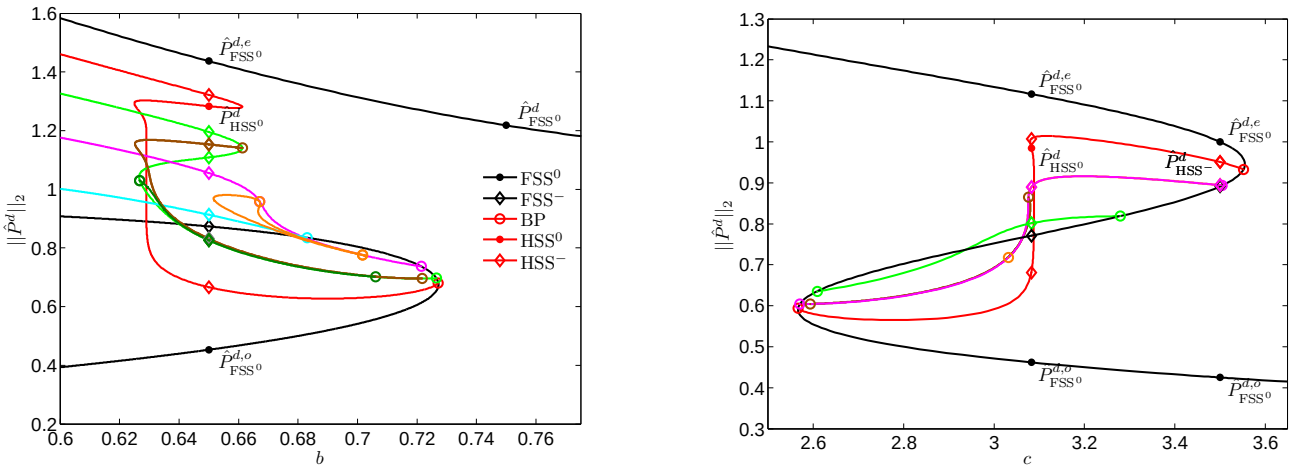

(a) First Scenario b, $\rho = 0.03, c = 0.5$

(b) Second Scenario c, $\rho = 0.3, b = 0.55$

Figure 5: A bifurcation analysis for the canonical system Eq. (21) is depicted in (a) and (b). The symbols: • denote equilibria satisfying the SPP, ⋄ equilibria not satisfying the SPP and ∘ branching points of the equilibria manifold. The FOSS curves are black and the HOSS curves are colored. Along the red HOSS curve two fold bifurcations occur, the HOSS candidates between these fold bifurcations satisfy the SPP.

- None of the PCSS are optimal.
- The two FCSS^0 are optimal.
- The according basins of attractions are separated by an indifference threshold manifold.
- In Grass and Uecker [2015] we computed a homogeneous and patterned indifference threshold point. The homogeneous indifference threshold point coincides with the value of the indifference threshold point in model (16).

Next we explain in detail the calculation of a solution converging to an equilibrium satisfying SPP. Subsequently the necessary steps for the detection of an indifference threshold point are explained. Details for the calculation in `OCMat` can be found in Appendix B.

4.3 A locally optimal patterned equilibrium

To prove that PCSS^0 $(\hat{P}^d_{\text{PCSS}^0}, \hat{\lambda}^d_{\text{PCSS}^0})$, see Fig. 5a, is an optimal equilibrium we have to show that there exist no other solution $(P^d(\cdot), u^d(\cdot))$ with $P^d(0) = \hat{P}^d_{\text{PCSS}^0}$ yielding a larger objective value. There exist two other equilibria satisfying SPP, namely the two FCSS^0, the oligotrophic $(\hat{P}^{d,o}_{\text{FCSS}^0}, \hat{P}^{d,o}_{\text{FCSS}^0})$ and the eutrophic FCSS^0 $(\hat{P}^{d,e}_{\text{FCSS}^0}, \hat{\lambda}^{d,e}_{\text{FCSS}^0})$ (cf. Fig. 5a). For each of these equilibria there may exist a path with $P^d(0) = \hat{P}^d_{\text{PCSS}^0}$ and converging to the oligotrophic/eutrophic equilibrium. To determine these paths we consider the corresponding homotopy problems Eq. (25) with x_1 replaced by $\hat{P}^d_{\text{PCSS}^0}$, starting at the equilibrium $(\hat{P}^{d,o}_{\text{FCSS}^0}, \hat{P}^{d,o}_{\text{FCSS}^0})$ and $(\hat{P}^{d,e}_{\text{FCSS}^0}, \hat{\lambda}^{d,e}_{\text{FCSS}^0})$, respectively.

4.3.1 Comparison with equilibrium solution

The result of these computations is depicted in Fig. 6. Figure 6a illustrates the "embedding" Eq. (25b). The green manifold proceed from the flat eutrophic states $\hat{P}^{d,e}_{\text{FCSS}^0}$ and the blue manifold from the flat oligotrophic states $\hat{P}^{d,o}_{\text{FCSS}^0}$ to the patterned states $\hat{P}^d_{\text{PCSS}^0}$. During the continuation of κ from zero to

one the initial states lie in these manifolds. In Figs. 6b and 6c the states and their norm of the solution paths for $\kappa = 0.5$ are shown (green and blue). Additionally the states and norm of the equilibrium solution $\hat{P}^d_{\mathrm{PCSS}^0}$ are depicted.

Figures 6d to 6f display the final results for $\kappa = 1$ also including the figure with the control paths. Moreover, Fig. 6g and Fig. 6e reveal that the values of the costates and hence the controls of the three solutions with $P^d(0) = \hat{P}^d_{\mathrm{PCSS}^0}$ are different.

Figure 6h show the slice manifolds (see Definition A.1) in the state-costate space. Each marker $\times$ denotes a continuation step.

In Fig. 6e the objective values along the slice manifolds are plotted, i.e. the objective values are plotted against the (norm) of the initial points. We see that the final solutions for $\kappa = 1$ both yield a higher objective value and the eutrophic solution converging to $\mathrm{FCSS}^0{}_2$ dominates the other solutions. On the other hand the gradients of the curves suggest that they eventually intersect. Such an intersection point characterizes an indifference threshold point (cf. Fig. 3b for the 0D model).

4.3.2 Detection and Continuation of an indifference threshold point ITP

To find a possible intersection point of the objective values along the slice manifolds we have to assure that the slice manifolds are comparable and have to check if they intersect (see Definition A.2). The slice manifolds depicted in Fig. 6h are, e.g., not comparable, simply because the manifolds

$$\{\hat{P}^{d,o}_{\mathrm{FCSS}^0} + (1-\alpha_1)(\hat{P}^d_{\mathrm{PCSS}^0} - \hat{P}^{d,o}_{\mathrm{FCSS}^0}) : \ \alpha_1 \in \mathbb{R}\}$$
$$\{\hat{P}^{d,e}_{\mathrm{FCSS}^0} + (1-\alpha_2)(\hat{P}^d_{\mathrm{PCSS}^0} - \hat{P}^{d,e}_{\mathrm{FCSS}^0}) : \ \alpha_2 \in \mathbb{R}\}.$$

are different. See Fig. 6a), where the green and blue curves depict (parts) of these manifolds. Only if slice manifolds are comparable and have a non-empty intersection this means that the solutions corresponding to the intersection points of the slice manifold start at the same initial states and hence their objective values can be compared.

Anyhow, since the solution starting at $\hat{P}^d_{\mathrm{PCSS}^0}$ and converging to $\mathrm{FCSS}^0{}_2$ is known we can start the homotopy BVP (25) with

$$X(0) = \hat{P}^d_{\mathrm{PCSS}^0} + (1-\kappa)(\hat{P}^{d,o}_{\mathrm{FCSS}^0} - \hat{P}^d_{\mathrm{PCSS}^0}).$$

In that case the manifolds

$$\{\hat{P}^{d,o}_{\mathrm{FCSS}^0} + (1-\alpha_1)(\hat{P}^d_{\mathrm{PCSS}^0} - \hat{P}^{d,o}_{\mathrm{FCSS}^0}) : \ \alpha_1 \in \mathbb{R}\}$$
$$\{\hat{P}^d_{\mathrm{PCSS}^0} + (1-\kappa)(\hat{P}^{d,o}_{\mathrm{FCSS}^0} - \hat{P}^d_{\mathrm{PCSS}^0}) : \ \kappa \in \mathbb{R}\}.$$

trivially coincide and the slice manifolds are comparable, see Fig. 7a. Moreover the slice manifolds intersect and and the corresponding objective values curves intersect at an indifference threshold point $P^d_{I,1}$ (cf. Fig. 7d).

In Fig. 7b and Fig. 7e the corresponding state $P^d_{e,o}(\cdot)$ and control paths $u^d_{e,o}(\cdot)$) are shown.

Repeating the same procedure for the three two FCSS^0 and PCSS^0 we find that PCSS^0 is not optimal and again we find a further indifference threshold point $P^d_{I,2}$. The according solutions are depicted in Fig. 7c and Fig. 7f.

It is an interesting question to see how we can find indifference threshold points "between" $P^d_{I,1}$ and $P^d_{I,2}$. Let us recall that we found the indifference threshold points by the intersection of two n dimensional manifolds (with $n = N+1$ the number of states P^d) in the $n+1$ dimensional space $(P^d, J(P^d(0)))$. Generically this yields an $n-1 = N$ dimensional manifold. Already for the discretization $N = 50$ its dimension is too large to recover the entire indifference threshold manifold (in the original PDE problem the dimension actually increases to infinity). Anyhow, we can e.g. search for indifference threshold points along the linear connection $P^d_{I,2} + (1-\kappa)(P^d_{I,1} - P^d_{I,2})$. The result is depicted in an animation embedded into Fig. 7e. The according BVP for the numerical solution of this problem is presented in Appendix A.2.2.

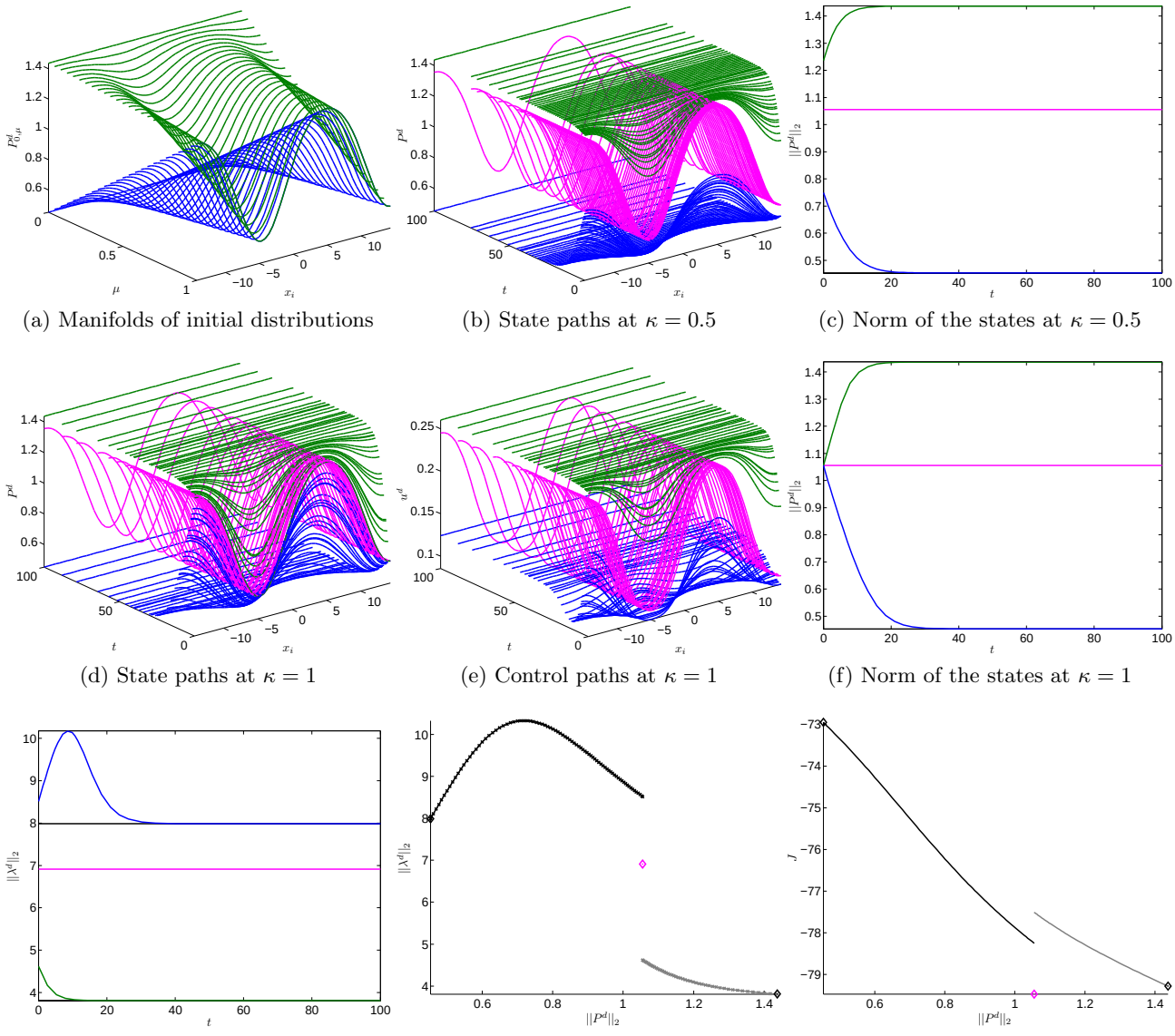

(a) Manifolds of initial distributions (b) State paths at $\kappa = 0.5$ (c) Norm of the states at $\kappa = 0.5$

(d) State paths at $\kappa = 1$ (e) Control paths at $\kappa = 1$ (f) Norm of the states at $\kappa = 1$

(g) Norm of the costates at $\kappa = 1$ (h) Slice manifolds (i) Objective values at slice manifolds

Figure 6: This figure presents the steps of the continuation process to find solutions starting at $P^d(0) = \hat{P}^d_{\text{PCSS}^0}$ and converging to the oligotrophic and eutrophic FCSS^0. The colors refer to the eutrophic (blue), oligotrophic (green) and patterned (magenta) solutions. In (a) the manifolds of initial distributions, that are passed through the continuation, are depicted. For the continuation parameter $\kappa = 0.5$ the state paths and corresponding norms are shown in (b) and (c). The final results are illustrated in (d) (state paths), (e) (control paths), (f) (costate paths), and (g) (norms). In (h) the corresponding slice manifolds are shown in the state-costate space. The objective values for solutions of the slice manifolds in (i) show that the path converging to the oligotrophic equilibrium is optimal among all solutions that start in $P^d(0) = \hat{P}^d_{\text{PCSS}^0}$.

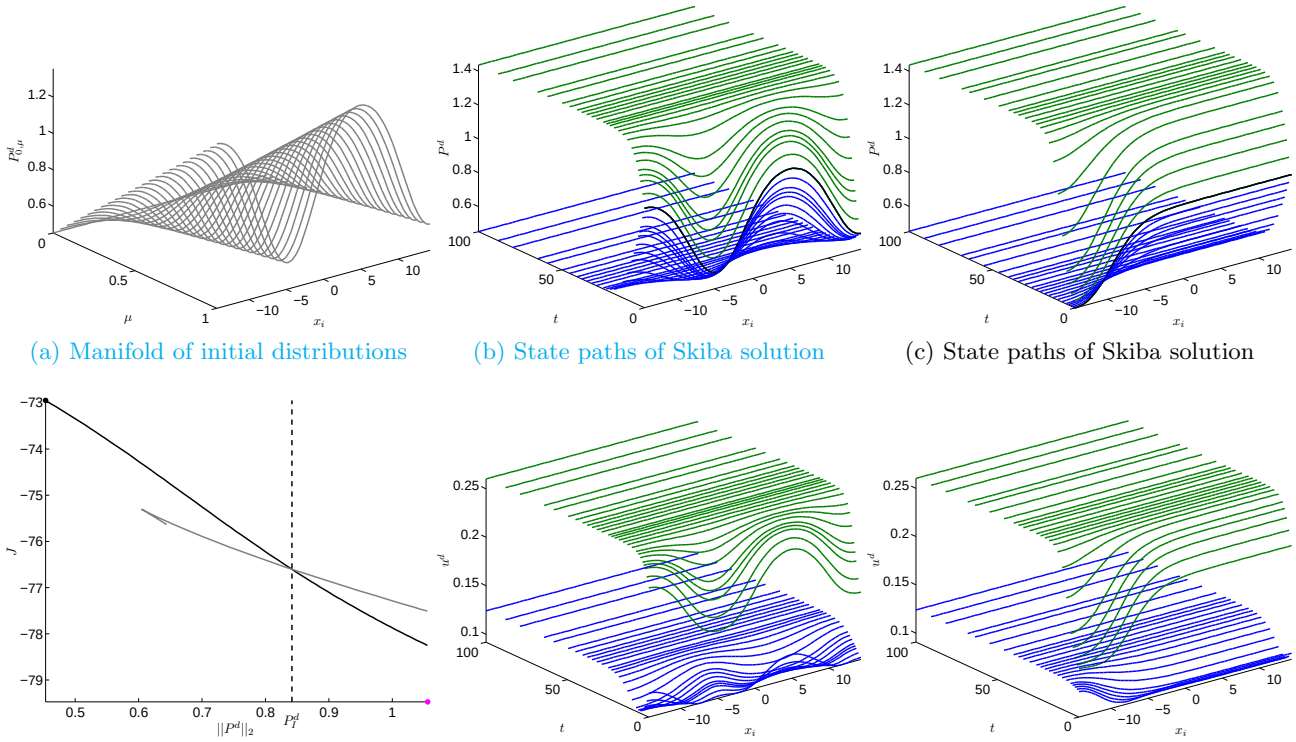

(a) Manifold of initial distributions (b) State paths of Skiba solution (c) State paths of Skiba solution

(d) Crossing of objective values (e) Control paths of Skiba solution (f) Control paths of Skiba solution

Figure 7: This figure shows the detection of a patterned Skiba distribution and its continuation to a different Skiba distribution on the Skiba manifold. To receive the animation files associated to the panels (a), (b) and (e) please contact the author.

4.4 Second scenario

In the first scenario with $b = 0.65$ we only found the eutrophic and oligotrophic equilibria being FOSS. This is somehow analogous to the 0D model, where the CSS does not appear in the optimal system (see Fig. 3).

The result for the 0D model in the second scenario shows that beside the eutrophic and oligotrophic CSS^0 the unstable node (CSS^-) appears as limit of the regions of attractions for the two CSS^0. Thus, we can expect that FCSS^- is optimal in model (20). Therefore, also PCSS^- cannot be excluded to be optimal.

We therefore analyze two different cases with $c = 3.5$ where none of the PCSS satisfy SPP and $c = 3.0825$, for which one of the PCSS satisfies SPP. For the original shallow lake model (16) these two cases are qualitatively the same (cf. Fig. 4).

4.4.1 Patterned equilibrium not satisfying SPP

For $c = 3.5$ we try to find solutions that start at the states of the FCSS^- ($\hat{P}^d_{\mathrm{FCSS}^-}$) and one of the PCSS^- and converge to the eutrophic (oligotrophic) FCSS.

In Fig. 8 the main results of this analysis are depicted. The example depicted in the first column (a,d and g) is analogous to the case in the 0D model shown in Fig. 4. Thus, it is not possible to find a solution starting at the initial states of the FCSS^- and converging to the eutrophic or oligotrophic FCSS. Instead, during the continuation process the initial states of $\hat{P}^d_{\mathrm{FCSS}^-}$ are approached but cannot be reached. In Fig. 8a the phase portrait of the final result is plotted, which is analogous to the state-costate space in 0D (cf. Fig. 4a). In Fig. 8c we see that the objective value for the homogeneous initial distributions is continuous (cf. Fig. 4b). Consequently, for spatially homogeneous initial distributions, the optimal path is unique, where $\hat{P}^d_{\mathrm{FCSS}^-}$ separates the regions of attractions for the eutrophic (oligotrophic) equilibrium $\hat{P}^{d,e}_{\mathrm{FCSS}^0}$ ($\hat{P}^{d,o}_{\mathrm{FCSS}^0}$). The optimal state paths for solutions starting exactly at $\hat{P}^d_{\mathrm{FCSS}^-}$ (the equilibrium solution, black) and in the near vicinity (blue and green) are depicted in Fig. 8d. Repeating these steps for each of the PCSS, two examples are depicted in the last two columns of Fig. 8, yields that each of these equilibria is optimal, i.e. are POSS. Since none of the PCSS satisfy SPP these equilibria and their stable manifolds separate the regions of attractions of the FOSS.

At this point a few questions remain unsettled.

- Is the defect of an equilibrium not satisfying SPP constant for state discretizations that are fine enough?
- What does this mean for the original PDE problem?
- Can we say that equilibria not satisfying SPP and their stable manifolds separate the regions of attractions for the solutions satisfying SPP?
- What is the state space of the PDE problem?

4.4.2 Patterned equilibrium satisfying SPP

In this section we numerically check, whether the unique patterned equilibrium PCSS^0 for $c = 3.0825$ is POSS(cf. Fig. 5b). For that reason we have to show that there exists no other solution path of the canonical system Eq. (21) that starts at $\hat{P}^d_{\mathrm{PCSS}^0}$ yielding a larger objective value. The only other candidates are stable paths of the eutrophic and oligotrophic FCSS^0. The result of the numerical comparison for the oligotrohic versus the patterned equilibrium is depicted in Fig. 9d and Fig. 9e.

To find a feasible path $(P^d_1(\cdot,\kappa), \lambda^d_1(\cdot,\kappa))$ that satisfies $P^d(0,1) = \hat{P}^d_{\mathrm{PCSS}^0}$ and

$$\lim_{t\to\infty} (P^d_1(t,\kappa), \lambda^d_1(t,\kappa)) = (\hat{P}^{d,o}_{\mathrm{FCSS}^0}, \hat{P}^{d,o}_{\mathrm{FCSS}^0}) \quad \text{with} \quad \kappa \in [0,1]$$

we solve the homotopy problem Eq. (25), starting with the constant equilibrium solution $(\hat{P}^{d,o}_{\mathrm{FCSS}^0}, \hat{P}^{d,o}_{\mathrm{FCSS}^0})$. The continuation process revealed that it is not possible to find a feasible path for $\kappa = 1$, instead some value $\kappa_0 < 1$ was approached. The last computed path $(P_1^d(\cdot,\kappa_0), \lambda_1^d(\cdot,\kappa_0))$ is shown in Fig. 9a together with the corresponding slice manifold (dashed black).

Next we repeated the procedure for the reversed homotopy problem, starting with the constant patterned solution $(\hat{P}^d_{\mathrm{PCSS}^0}, \hat{\lambda}^d_{\mathrm{PCSS}^0})$ and trying to find a feasible path $(P_2^d(\cdot,1-\kappa), \lambda_2^d(\cdot,1-\kappa))$ that satisfies $P^d(0,0) = \hat{P}^{d,o}_{\mathrm{FCSS}^0}$ and

$$\lim_{t\to\infty} (P_2^d(t,1-\kappa), \lambda_2^d(t,1-\kappa)) = (\hat{P}^d_{\mathrm{PCSS}^0}, \hat{\lambda}^d_{\mathrm{PCSS}^0}) \quad \text{with} \quad \kappa \in [0,1].$$

Again the continuation process revealed that it was not possible to find a feasible path for $\kappa = 0$, instead some value approximately $1-\kappa_0$ was approached. This solution $(P_2^d(\cdot,1-\kappa), \lambda_2^d(\cdot,1-\kappa))$ is represented in Fig. 9b by the blue solution path and black slice manifold.

The two last solution paths from both continuation processes suggest that there exists a separating manifold for the regions of attractions of the oligotrophic FCSS^0 and PCSS^0. A possible candidate for this separating manifold is the stable manifold of the PCSS^- with defect -1 (see the $\diamond$ in Fig. 9c). To test this conjecture we solved the homotopy problem Eq. (29) for defective equilibria. For $x_1^{(1)}$ we took $P_1^d(0,\kappa_0)$ (the initial states of the last continuation step of the first homotopy problem) and set $V_1 := (1,\dots,1) \in \mathbb{R}^{N+1}$, which satisfies the rank condition Eq. (29d). The last solution $(P_3^d(\cdot,1), \lambda_3^d(\cdot,1))$ of this homotopy problem is depicted as dashed blue curve in Fig. 9d and gives a strong numerical argument for our conjecture.

The overall picture, Fig. 9d, suggests that for every $\varepsilon > 0$ there exists κ_1 and κ_2 such that there exists solutions $(P_1^d(\cdot,\kappa_1), \lambda_1^d(\cdot,\kappa_1))$ and $(P_2^d(\cdot,1-\kappa_2), \lambda_2^d(\cdot,1-\kappa_2))$ of the homotopy problems with

$$\|(P_1^d(0,\kappa_1), \lambda_1^d(0,\kappa_1)) - (P_3^d(0,1), \lambda_3^d(0,1))\|_2 < \varepsilon$$

and

$$\|(P_2^d(0,1-\kappa_2), \lambda_2^d(0,1-\kappa_2)) - (P_3^d(0,1), \lambda_3^d(0,1))\|_2 < \varepsilon$$

or even stronger

$$\|(P_1^d(\cdot,\kappa_1), \lambda_1^d(\cdot,\kappa_1)) - (P_3^d(\cdot,1), \lambda_3^d(\cdot,1))\|_{L_2} < \varepsilon$$

and

$$\|(P_2^d(\cdot,1-\kappa_2), \lambda_2^d(\cdot,1-\kappa_2)) - (P_3^d(\cdot,1), \lambda_3^d(\cdot,1))\|_{L_2} < \varepsilon.$$

Plotting the objective values evaluated along the solutions of the corresponding slice manifolds shows that the objective function is continuous in the vicinity of $P_3^d(0,1)$, see Fig. 9e. An analogous result holds for the comparison of the stable paths converging to the eutrophic FCSS^0 and the PCSS^0. This proves the optimality of FCSS^0 and PCSS^0 as well. Also according to the case $c = 3.5$ the stable manifolds of defective equilibria separate the regions of attractions of the equilibria satisfying SPP.

Figure 9f shows (part of) a phase portrait in the state-costate space for $c = 3.0825$. The subscripts of the equilibria denote the defect of the according equilibrium. Thus, there exist two FCSS^0 ($\hat{P}^{d,e}_{\mathrm{FCSS}^0}$ and $\hat{P}^{d,o}_{\mathrm{FCSS}^0}$), and one PCSS^0 ($\hat{P}^d_{\mathrm{PCSS}^0}$). Additionally a few paths are plotted that converge to $\hat{P}^{d,e}_{\mathrm{FCSS}^0}$, $\hat{P}^{d,o}_{\mathrm{FCSS}^0}$, and $\hat{P}^d_{\mathrm{PCSS}^0}$ (solid blue) and to PCSS^- with defect -1 (dashed blue). The specific case for solutions that converge to the oligotrophic equilibrium $(\hat{P}^{d,o}_{\mathrm{FCSS}^0}, \hat{P}^{d,o}_{\mathrm{FCSS}^0})$ and patterned equilibrium $(\hat{P}^d_{\mathrm{PCSS}^0}, \hat{\lambda}^d_{\mathrm{PCSS}^0})$ is separately illustrated in Fig. 9d and Fig. 9e.

5 Conclusion

The purpose of this article is the presentation of a numerical framework, that allows us to numerically experiment with 1D spatially distributed optimal control problems. Numerical experiment is meant in the sense of Heaviside, who claimed mathematics as an experimental science, cf. Heaviside [1893].

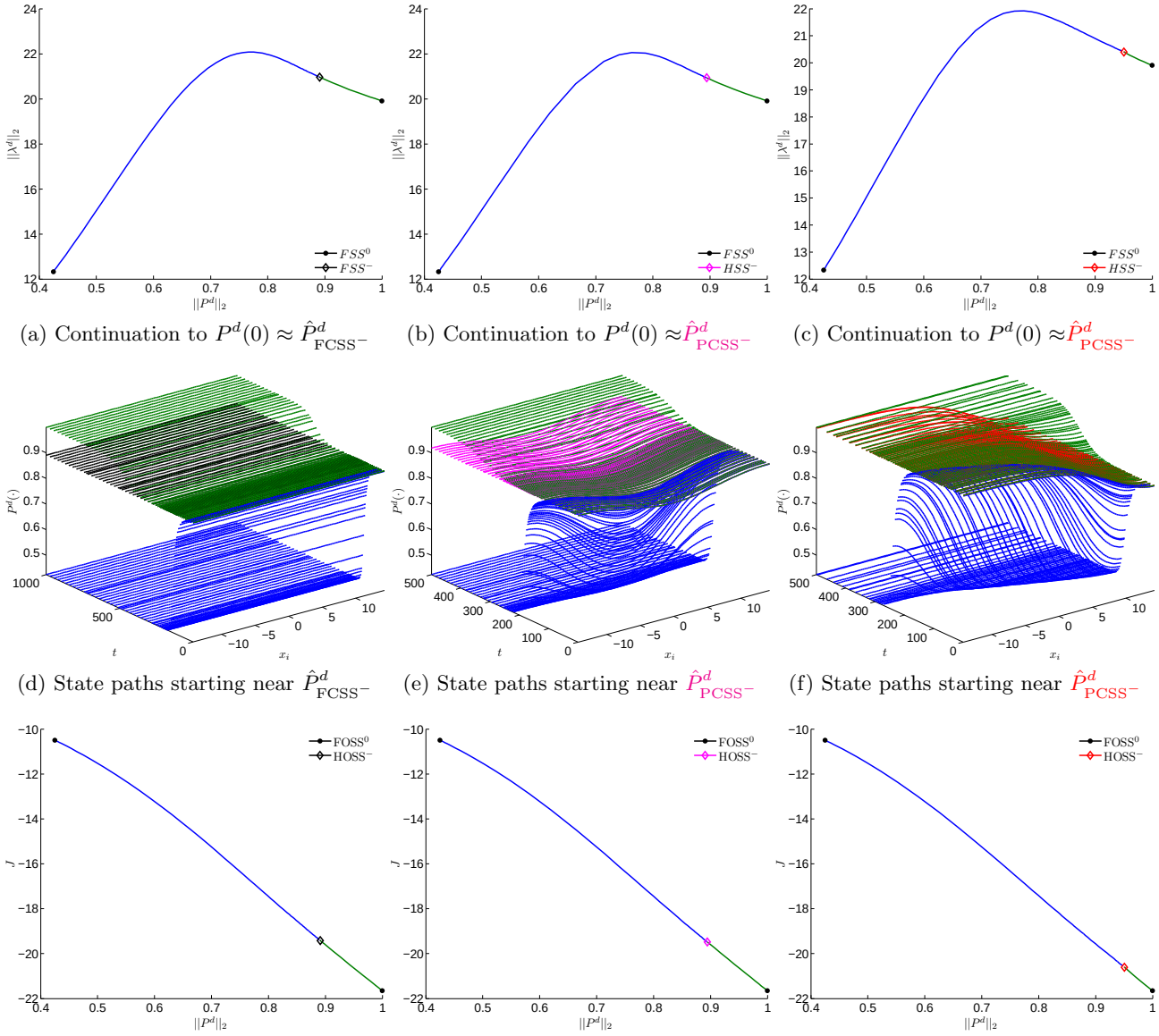

(a) Continuation to $P^d(0) \approx \hat{P}^d_{\text{FCSS}^-}$ (b) Continuation to $P^d(0) \approx \hat{P}^d_{\text{PCSS}^-}$ (c) Continuation to $P^d(0) \approx \hat{P}^d_{\text{PCSS}^-}$

(d) State paths starting near $\hat{P}^d_{\text{FCSS}^-}$ (e) State paths starting near $\hat{P}^d_{\text{PCSS}^-}$ (f) State paths starting near $\hat{P}^d_{\text{PCSS}^-}$

(g) Objective value along slice manifolds (h) Objective value along slice manifolds (i) Objective value along slice manifolds

Figure 8: This figure depicts the numerical proof for the optimality of FCSS$^-$ and PCSS$^-$ at $c = 3.5$, i.e., the optimality of the equilibria that do not satisfy SPP, exemplified for three equilibria. In the first row (a)-(c) the slice manifolds for the according continuation processes are depicted in the normed state-costate space. The second row (d)-(f) shows the state paths for the solutions starting at and near the FCSS$^-$ and PCSS$^-$, respectively. The last row (g)-(i) illustrates that the objective function is continuous in the vicinity of the constant equilibria solutions for the FCSS$^-$ and PCSS$^-$. Therefore the equilibria not satisfying SPP are optimal as well.

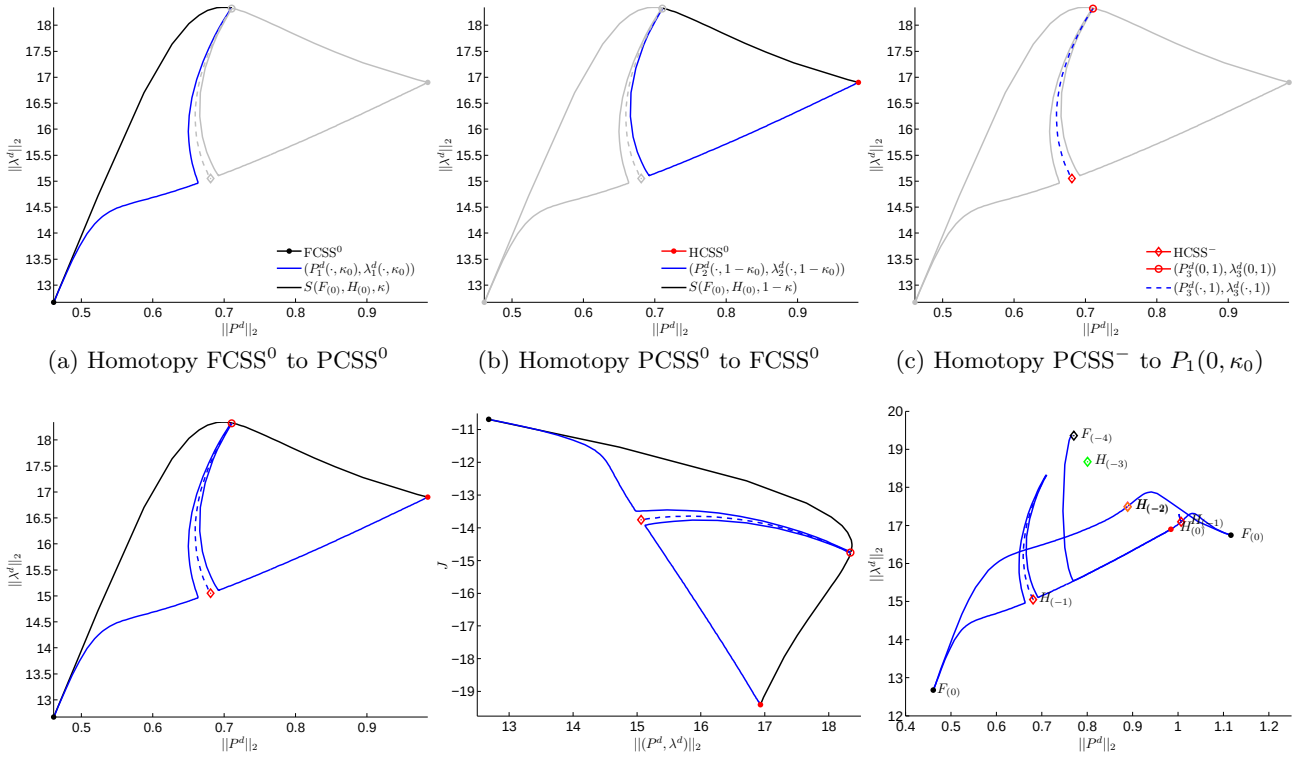

(a) Homotopy FCSS^0 to PCSS^0 (b) Homotopy PCSS^0 to FCSS^0 (c) Homotopy PCSS$^-$ to $P_1(0,\kappa_0)$

(d) Slice manifolds and solution paths (e) Objective value (f) Phase portrait

Figure 9: In (f) some of the solutions paths and equilibria in the state-costate space are depicted. The solutions shown in (d) and (e) are the result of the continuation processes, when we tried to find a solution starting at the states of POSS and converging to the oligotrophic FOSS, and vice versa. The continuation process approached a state lying on the stable manifold (dashed blue) of the PCSS$^-$ with defect -1. Thus, for initial states coinciding with the states of the stable manifold with defect -1 it is optimal to converge along the stable manifold to the POSS with defect -1. In the vicinity of these initial states it is optimal to converge either to the oligotrophic FOSS or the POSS satisfying SPP. To receive the animation file associated to the panel (d) please contact the author.

We were thus able to find numerical evidence for the occurrence of (indifference) threshold distributions in distributed models. Moreover, this points towards a possible generalization of the saddle point property, which in case of multiple canonical steady states (CSS) is intimately connected to the existence of multiple optimal solutions. Even though this simple FDM could also be applied to spatially 2D models, such an approach would immediately become numerically intractable. Therefore, it is an intermediate step to the method of a finite element discretization, that is presented in Grass and Uecker [2015] and extended in Uecker [2015].

Different directions for further research result from the presented approach. The obvious next step is the previously mentioned application of FEM discretization. This is realized as an add-on toolbox (`p2pOC`) to the MATLAB package `pde2path`, which is a numerical tool for continuation and bifurcation in 2D elliptic systems, cf. Uecker et al. [2014].[3]

A main drawback of the actual approach is difficulty to handle (inequality) constraints. For a correct usage of the used BVPsolver the rhs of the dynamics has to at least continuously differentiable. This property is violated, when constraints become active. We solved that problem by considering different arcs of the solution path, where each of the arcs satisfied the differentiability condition. For non-distributed models this is in general a practicable way but hardly to realize for distributed models. Simply because for each transition from one arc to the other the according switching conditions have to be stated. This ansatz quickly becomes intractable for the high dimensional discretized system.

Therefore, we will put effort in the development of a solver based on finite element discretization and conjugate gradient method combined with a continuation step.

A Numerical method implemented in `OCMat`

In this section we formulate the basic method for the calculation of paths that converge to an equilibrium of the canonical system.

A.1 The core problem

The core problem that has to be solved is the following. Given an equilibrium $(\hat{x}, \hat{\lambda})$ and an initial distribution x_0 we want to find a path $(x(\cdot), \lambda(\cdot))$ satisfying Eq. (3) together with the boundary conditions

$$x(0) = x_0 \quad \text{and} \quad \lim_{t\to\infty} (x(t), \lambda(t)) = (\hat{x}, \hat{\lambda}). \tag{22}$$

The dimension of the according eigenspace

$$0 < \dim \mathrm{E}^s(\hat{x}, \hat{\lambda}) = n_s \leq n.$$

Then, the boundary condition at infinity in Eq. (22) can be approximated by the so called asymptotic boundary condition [cf. Lentini, 1978, Lentini and Keller, 1980]

$$\Omega^\top \left(\begin{pmatrix} \hat{x} \\ \hat{\lambda} \end{pmatrix} - \begin{pmatrix} x(T) \\ \lambda(T) \end{pmatrix} \right) = 0 \in \mathbb{R}^{2n-n_s}, \quad \Omega \in \mathbb{R}^{2n\times(2n-n_s)} \quad \text{and} \quad \Omega \perp \mathrm{E}^s(\hat{x}, \hat{\lambda}) \tag{23}$$

with $T > 0$ large enough.

For a compact notation we introduce

$$X := \begin{pmatrix} x \\ \lambda \end{pmatrix} \quad \text{and Eq. (21) is written as} \quad \dot{X}(t) = F(X(t)).$$

[3] It can be downloaded for free from http://www.staff.uni-oldenburg.de/hannes.uecker/pde2path.

Then the previous BVP writes as

$$\dot{X}(t) = TF(X(t)), \quad t \in [0,1] \tag{24a}$$
$$X^{(i_1,\dots,i_{n_s})}(0) = x_0^{(i_1,\dots,i_{n_s})} \tag{24b}$$
$$\Omega^\top(\hat{X} - X(1)) = 0. \tag{24c}$$

If $\hat{X}$ satisfies SPP then $n_s = n$ and Eq. (24b) simplifies to $X^{(1,\dots,n)}(0) = x_0$. To keep notation simple we assume that the coordinates of x are sorted, such that $(i_1,\dots,i_{n_s}) = (1,\dots,n_s) =: (n_s)$. Then Eq. (24b) can be rewritten as

$$X^{(n_s)}(0) = x_0^{(n_s)} \tag{24b'}$$

In general BVP (24) cannot be solved analytically, hence numerical methods have to be applied. These numerical methods request some initial function $\tilde{X}(\cdot)$. Such an initial function need not satisfy the BVP (24) but, depending on the problems properties, it has to a more or less good approximation. What can we do if such an initial function is not at hand?

A.2 Embedding into a homotopy problem

Given that a solution $Y(\cdot)$ of Eq. (24) with $Y^{(n)}(0) = x_1^{(n)} \neq x_0^{(n)}$ is available we can embed Eq. (24) into the according homotopy problem

$$\dot{X}(t) = TF(X(t),\mu), \quad t \in [0,1] \tag{25a}$$
$$X^{(n)}(0) = x_0^{(n)} + (1-\kappa)(x_1^{(n)} - x_0^{(n)}) \tag{25b}$$
$$\Omega^\top(\hat{X} - X(1)) = 0. \tag{25c}$$

Then $Y(\cdot)$ solves Eq. (25) for $\kappa = 0$ and $\kappa = 1$ yields a solution of BVP (24). `OCMat` solves the homotopy BVP (25) using arclength continuation [Kuznetsov, 1998, Allgower and Georg, 2003]. Thus, at each homotopy step $i > 0$ with previous solution $(X_{(i-1)}(\cdot), \kappa_{i-1})$ the BVP (25) is solved for $(X_{(i)}(\cdot), \kappa_i)$ together with the additional equation

$$\int_0^1 (X_{(i)}(t) - X_{(i-1)}(t))^\top V_{(i-1)}(t)\mathrm{d}t + (\kappa_i - \kappa_{i-1})V_{(i-1),\kappa} = 0 \tag{25d}$$

where $(V_{(i-1)}(\cdot), V_{(i-1),\kappa})$ satisfies the linearized BVP

$$\dot{V}_{(i-1)}(t) = TF_X(X_{(i-1)}(t),\mu)V_{(i-1)}(t), \quad t \in [0,1] \tag{25e}$$
$$V_{(i-1)}^{(n)}(0) = V_{(i-1),\kappa}(x_1^{(n)} - x_0^{(n)}) \tag{25f}$$
$$\Omega^\top V(1) = 0. \tag{25g}$$

The solution $(V_{(i-1)}(\cdot), V_{(i-1),\kappa})$ of BVP (25e)–(25g) is called the *tangent* solution at step $i-1$. In the actual `OCMat` implementation the BVP (25a)–(25g) is discretized providing different discretization schemes, relying on the two native MATLAB BVP solvers `bvp4c`, `bvp5c` [cf. Kierzenka and Shampine, 2001, 2008], and the adapted solver `bvp6c` [cf. Hale, 2006, Hale and Moore, 2008]. The discretized tangent is computed at each Newton step. This is a specific arclength continuation, called Moore-Penrose continuation, cf. Kuznetsov [1998].

Subsequently we introduce some terminology to make a clear distinction between the stable paths and the set of initial points computed during a continuation process.

Definition A.1 (Slice Manifold)**.** *Let $X(\cdot,\kappa(s))$, $s \in I \subset \mathbb{R}$ with I a non-empty interval and $\kappa(\cdot) \in C^0(I,\mathbb{R})$ be a solution of Eq. (25) for every $s \in I$. Then*

$$S(\hat{X}, x_0^{(n_s)}, x_1^{(n_s)}, \kappa(\cdot)) := \{X(0,\kappa(s)) : \ s \in I\} \tag{26}$$

is called the slice manifold *along $x_0^{(n_s)}, x_1^{(n_s)}$ for $\hat{X}$ and $\kappa(\cdot)$.*

Definition A.2 (Comparable Slice Manifolds)**.** *Let $\hat{X}$ satisfy SPP and $S(\hat{X}_j, x_0^j, x_1^j, \kappa_j(s_j))$, $s_j \in I_j$, $j = 1,2$ be two slice manifolds along x_0^j, x_1^j for $\hat{X}_j$ and $\kappa_j(\cdot)$ with $x_0^j \neq x_1^j$, $j = 1,2$. Then $S(\hat{X}_j, x_0^j, x_1^j, \kappa_j(s_j))$, $j = 1,2$ are called* comparable *iff*

$$\{x_0^1 + (1-\alpha_1)(x_1^1 - x_0^1) : \ \alpha_1 \in \mathbb{R}\} = \{x_0^2 + (1-\alpha_2)(x_1^2 - x_0^2) : \ \alpha_2 \in \mathbb{R}\} \tag{27}$$

holds.

If comparable slice manifolds satisfy

$$\{x_0^1 + (1-\kappa_1(s))(x_1^1 - x_0^1) : \ s \in I_1\} \cap \{x_0^2 + (1-\kappa_2(s))(x_1^2 - x_0^2) : \ s \in I_2\} \neq \emptyset \tag{28}$$

it is said that the slice manifolds are intersecting.

Remark A.1. *A slice manifold is a linear cut through the stable manifold. At the intersection of two different slice manifolds the cuts are given for the same (initial) states x_0. Hence the according paths are (different) solution candidates for the optimal control problem with $x(0) = x_0$. For one state autonomous optimal control problems with the stable path $(x(\cdot),\lambda(\cdot))$ converging to $(\hat{x},\hat{\lambda})$*

$$S(x_0, x(T), \hat{x}, \mathrm{id}_{[0,1]}) = \{(x(t),\lambda(t)) : \ t \in [0,T]\}.$$

Thus, the orbit of the stable path coincides with the stable manifold. Moreover two slice manifolds for different saddles are trivially comparable.

There are good reasons to consider BVP (25) instead of BVP (24). For an arbitrary initial point x_0 it is often hard to provide a "good" guess of an initial function for BVP (24). Since in general the solution of an BVP is not unique it may not be guaranteed that a computed solution is the searched for solution.

On the other hand the equilibrium solution trivially satisfies BVP (24) for the initial point $\hat{x}$. Hence the homotopy BVP (25) can be started with an exact solution. Then the existence of a unique solution is guaranteed by the implicit function theorem as long as some rank condition is satisfied. A careful inspection of the linearization of BVP (25), which is a byproduct of the arclength continuation, then yields important information about the behavior of the solution paths. Moreover, these intermediate solution paths can be used to find, e.g. an indifference threshold point.

A.2.1 The stable manifold for an equilibrium not satisfying SPP

In the previous section we assumed that $\hat{X}$ satisfies SPP, i.e., $\dim \mathrm{E}^s(\hat{J}) = n$. Next we adapt BVP (25) for the case $\dim \mathrm{E}^s(\hat{J}) = n_s < n$. Therefore, we assume that $\hat{X}$ is hyperbolic with $\dim \mathrm{E}^u(\hat{J}) = n_u$ and hence $2n = n_s + n_u$. Furthermore, two points $x_i^{(n)}$ in the state space are fixed and $n - n_s$ vectors $v_i \in \mathbb{R}^n$ are chosen. Then, the according BVP for the calculation of stable paths converging to $\hat{X}$ becomes

$$\dot{X}(t) = TF(X(t),\mu), \quad t \in [0,1] \tag{29a}$$

$$X^{(n)}(0) = x_1^{(n)} + (1-\kappa_0)(x_0^{(n)} - x_1^{(n)}) + \sum_{i=1}^{n-n_s} \kappa_i v_i \tag{29b}$$

$$\Omega^\top(\hat{X} - X(1)) = 0 \in \mathbb{R}^{n_u} \tag{29c}$$

with

$$\begin{aligned} &\operatorname{rank}\left((x_0^{(n)} - x_1^{(n)}) \quad v_1 \quad \cdots \quad v_{n-n_s}\right) = n - n_s + 1 \\ &\Omega \perp \mathrm{E}^s(\hat{J}) = 0 \quad \text{and} \quad \Omega \in \mathbb{R}^{2n \times n_u}. \end{aligned} \tag{29d}$$

Let us assume that a solution $Y(\cdot)$ for $\kappa_j = 0,\ j = 0, \dots, n - n_s$ is known. Then Eq. (29b) can be interpreted as the condition that we search for a solution along the direction $x_0^{(n)} - x_1^{(n)}$. Additionally we have to take care letting enough freedom, guaranteed by 29d, to start at the stable manifold.

A.2.2 Continuation of an indifference threshold point

A useful relation between the Hamiltonian and objective value is given for a model (1) with $\rho > 0$ and finite objective value [cf. Michel, 1982]. Then we find for any solution $x(\cdot), \lambda(\cdot)$ of the canonical system Eq. (3)

$$J(x_0) = \frac{1}{\rho}\mathcal{H}(x(0), \lambda(0)) \tag{30}$$

where $\mathcal{H}$ is defined according to Eq. (3d) and the bar is omitted.

Let $\hat{Y}_i,\ i = 1, 2$ be two CSS of Eq. (3) and x_I^1 and x_I^2 be two distinct indifference threshold points of model (1). Furthermore, let $Z_{1,2}(\cdot)$ be two solutions corresponding to x_I^1 and $Z_{3,4}(\cdot)$ two solutions corresponding to x_I^2. To continue the indifference threshold point from x_I^1 to x_I^2 we solve the following homotopy problem

$$\dot{X}_1(t) = T_1 F(X_1(t)), \quad t \in [0, 1] \tag{31a}$$
$$\dot{X}_2(t) = T_2 F(X_2(t)), \quad t \in [0, 1] \tag{31b}$$
$$X_1^{(n)}(0) = X_2^{(n)}(0) \in \mathbb{R}^n \tag{31c}$$
$$\mathcal{H}(X_1(0)) - \mathcal{H}(X_2(0)) = 0 \in \mathbb{R} \tag{31d}$$
$$\Omega_1^\top(\hat{Y}_1 - X_1(1)) = 0 \in \mathbb{R}^n \tag{31e}$$
$$\Omega_2^\top(\hat{Y}_2 - X_2(1)) = 0 \in \mathbb{R}^n \tag{31f}$$
$$X_1^{(n)}(0) = x_I^2 + (1 - \kappa_1)(x_I^1 - x_I^2) + \kappa_2 V \in \mathbb{R}^n \tag{31g}$$

with

$$\begin{aligned} &a_1 V + a_2(x_I^1 - x_I^2) = 0 \quad \text{and} \quad |a_1| + |a_2| \neq 0 \\ &\Omega_i \perp \mathrm{E}^s(\hat{J}_i),\ i = 1, 2. \end{aligned}$$

Equations (31a) and (31b) denote the dynamics for the two distinct paths, starting at the same initial states, Eq. (31c). The truncation times $T_1 > 0$ and $T_2 > 0$ may be chosen differently. The two paths $X_1(\cdot)$ and $X_2(\cdot)$ yield the same objective value which according to Eq. (30) can be stated as Eq. (31d). Equations (31e) and (31f) denote the asymptotic boundary conditions for the path $X_1(\cdot)$ converging to $\hat{Y}_1$ and $X_2(\cdot)$ converging to $\hat{Y}_2$, respectively. Finally Eq. (31g) specifies the continuation in the state space, where the first part $x_I^2 + (1 - \kappa_1)(x_I^1 - x_I^2)$ describes the change into the direction to the target x_I^1 and $\kappa_2 V$ is a correction term, since the stable manifold has one dimension less than the state space.

Counting the number of unknowns and equations, we find $4n + 2$ unknowns, two times the states and costates $X_i(\cdot)$ and the two free parameters $\kappa_i,\ i = 1, 2$ and $4n + 1$ equations. Moreover Eq. (31) is solved for $(Z_{1,2}(\cdot), 0, 0)$ and $(Z_{3,4}(\cdot), 1, 0)$. Thus we can start a continuation process starting with one of these previously detected solutions.

B The usage of OCMat

In this section the basic steps for the numerical analysis of model (20) are explained in detail. This enables the user to reproduce the presented results and learn the basic commands and structure of OCMat.

B.1 The initialization file

To get results that are comparable smooth in the spatial dimension as the discretization used in Grass and Uecker [2015] we choose $N = 51$. In the syntax logic of OCMat we have to provide an initialization file consisting of $N + 1$ ODEs, the entry of $N + 1$ state and control variables $P_i, u_i, i = 0, \ldots, N$ and the appropriate objective function. Doing that by hand can become a boring and error-prone task. We therefore wrote a MATLAB file 'makeinitfile' that generates the initialization file, providing N[4]

```
function makeinitfile(N,modelname)

if nargin==1
    modelname='shallowlakeline';
end
dotPxi='uxi-b*Pxi+Pxi^2/(1+Pxi^2)+D*(N/2/L)^2*(Pxim1-2*Pxi+Pxip1)';
intvar='';
for ii=0:N
    ode{ii+1}=['DPx' num2str(ii) '=' strrep(strrep(strrep(strrep(dotPxi,'i',num2str(
   ii)),['x' num2str(ii) 'm1'],['x' num2str(ii-1)]),['x' num2str(ii) 'p1'],['x' num2str(ii
   +1)]),'Px-1','Px1'),['Px' num2str(N+1)],['Px' num2str(N-1)])];
    ode{ii+1}=char(simple(sym(ode{ii+1})));
    if ii>0
        controlvar=[controlvar ',ux' num2str(ii)];
        statevar=[statevar ',Px' num2str(ii)];
        if ii<N
            intvar=[intvar '+log(ux' num2str(ii) ')-c*Px' num2str(ii) '^2' ];
        else
            intvar=[intvar '+(log(ux0)-c*Px0^2+log(ux' num2str(ii) ')-c*Px' num2str(ii) '
   ^2)/2' ];
        end
    else
        controlvar=['ux' num2str(ii)];
        statevar=['Px' num2str(ii)];
    end
end
intvar(1)=[];
intvar=['(' char(collect(simple(sym(intvar)),'c')) ')'];

par={'rho::0.03','b::0.65','c::0.5','D::0.5','L::2*pi/0.44',['N::' num2str(N)]};
initfilefid=fopen([modelname '.ocm'],'w');
fprintf(initfilefid,'Type\nstandardmodel\n\nVariable\nstate::%s\ncontrol::%s\n\
   nStatedynamics\n',statevar,controlvar);
for ii=1:length(ode)
    fprintf(initfilefid,'ode::%s\n',ode{ii});
end
fprintf(initfilefid,'\nObjective\nexpdisc::rho\nint::%s\n\nParameter\n',intvar);
for ii=1:length(par)
```

[4] If this FDM approach turns out to be an important tool by itself, this step could be directly implemented within OCMat.

```
    fprintf(initfilefid,'%s\n',par{ii});
end
fclose(initfilefid);
```

As an example we call

```
>> makeinitfile(5,'shallowlakelinetest')
```

at the MATLAB workspace and the file `'shallowlakelinetest.ocm'` is generated

```
Type
standardmodel

Variable
state::Px0,Px1,Px2,Px3,Px4,Px5
control::ux0,ux1,ux2,ux3,ux4,ux5

Statedynamics
ode::DPx0=ux0-b*Px0+Px0^2/(1+Px0^2)+D*(N/2/L)^2*(Px1-2*Px0+Px1)
ode::DPx1=ux1-b*Px1+Px1^2/(1+Px1^2)+D*(N/2/L)^2*(Px0-2*Px1+Px2)
ode::DPx2=ux2-b*Px2+Px2^2/(1+Px2^2)+D*(N/2/L)^2*(Px1-2*Px2+Px3)
ode::DPx3=ux3-b*Px3+Px3^2/(1+Px3^2)+D*(N/2/L)^2*(Px2-2*Px3+Px4)
ode::DPx4=ux4-b*Px4+Px4^2/(1+Px4^2)+D*(N/2/L)^2*(Px3-2*Px4+Px5)
ode::DPx5=ux5-b*Px5+Px5^2/(1+Px5^2)+D*(N/2/L)^2*(Px4-2*Px5+Px4)

Objective
expdisc::rho
int::((-Px1^2-Px2^2-Px3^2-Px4^2-1/2*Px0^2-1/2*Px5^2)*c+log(ux1)+log(ux2)+log(ux3)+log(ux4)
   +1/2*log(ux0)+1/2*log(ux5))

Parameter
rho::0.03
b::0.65
c::0.5
D::0.5
L::2*pi/0.44
N::5
```

This file is placed at the actual MATLAB directory, to make it visible for `OCMat` it has to be moved to the folder `ocmat\model\initfiles`. After that the initialization process of `OCMat` can be started

```
>> ocStruct=processinitfile('shallowlakelinetest');
ocmat\model\usermodel\shallowlakelinetest does not exist. Create it?  (y)/n: y
ocmat\model\usermodel\shallowlakelinetest\data does not exist. Create it?  (y)/n: y
ocmat\model\usermodel\shallowlakelinetest\data is not on MATLAB path. Add it?  (y)/n: y
ocmat\model\usermodel\shallowlakelinetest is not on MATLAB path. Add it?  (y)/n: y
>> modelfiles=makefile4ocmat(ocStruct);
>> moveocmatfiles(ocStruct,modelfiles)
```

For the following analysis we use the initialization file `shallowlakelinecoarse` with $N = 51$. Thus, the previous initialization commands have to be repeated with `shallowlakelinecoarse` instead of `shallowlakelinetest`. Note that even though the discretization parameter N appears as a parameter of the model `shallowlakelinecoarse` it must not be changed. The initialization steps can be very time consuming, depending on the chosen value of N and the computer capacity. For $N = 51$ the initialization, on a PC with the specifications Intel Core i7-3820 CPU@3.60GHz, Windows 7, MATLAB 7.6.0, took around half an hour.

Subsequently we will also make use of the 0D shallow lake model. Therefore, we have to run through the initialization process for the model `shallowlake`[5] as well.

[5]The according initialization file `shallowlake.ocm` can be found in the folder `ocmat/mode/initfiles`.

```
>> ocStruct=processinitfile('shallowlake');
ocmat\model\usermodel\shallowlake does not exist. Create it?  (y)/n: y
ocmat\model\usermodel\shallowlake\data does not exist. Create it?  (y)/n: y
ocmat\model\usermodel\shallowlake\data is not on MATLAB path. Add it?  (y)/n: y
ocmat\model\usermodel\shallowlake is not on MATLAB path. Add it?  (y)/n: y
>> modelfiles=makefile4ocmat(ocStruct);
>> moveocmatfiles(ocStruct,modelfiles)
```

B.2 Detection and continuation of equilibria

For the calculation of the FCSS we use the equilibria of the `shallowlake` model. A detailed explanation of the commands can be found in the `OCMat` manual.

```
>> m0=stdocmodel('shallowlake');
>> m0=changeparametervalue(m0,'b,c',[0.65 0.5]);
>> ocEP0=calcep(m0);b=isadmissible(ocEP0,m0,[],'UserAdmissible');ocEP0(~b)=[];
```

The values of the equilibria are used to generate the values of FCSS.

```
>> m=stdocmodel('shallowlakelinecoarse');
>> N=parametervalue(m,'N');
>> y0=[ocEP0{1}.y([1 end]) ocEP0{2}.y([1 end]) ocEP0{3}.y([1 end])];
>> Y=[y0([ones(N+1,1);2*ones(N+1,1)],1) y0([ones(N+1,1);2*ones(N+1,1)],2) y0([ones(N+1,1)
   ;2*ones(N+1,1)],3)];
>> Y([N+2 2*N+2],:)=Y([N+2 2*N+2],:)/2;
>> opt=setocoptions('EQ','TolFun',1e-12,'MaxFunEvals',50000,'MaxIter',50000);
>> ocEP=calcep(m,Y,[],opt);b=isadmissible(ocEP,m);ocEP(~b)=[];
>> [b dfct]=isspp(m,ocEP{:})
b =
     1     0     1
dfct =
     0    -5     0
```

Thus, the first and third equilibrium satisfy SPP, the second equilibrium has defect -5. For the subsequent step an adapted version of `CL_MATCONT` has been used.

```
>> opt0=setocoptions('MATCONT','MaxNumPoints',750,'MaxStepsize',1e-1,'Backward',0,'
   IgnoreSingularity',2,'OCCONTARG','CheckAdmissibility','off');
>> opt1=setocoptions(opt0,'MATCONT','Backward',1);
>> contpar='b';epidx=1;[x0 v0 s0 f0 h0]=contep(m,ocEP{epidx},contpar,opt0);
first point found
tangent vector to first point found
elapsed time  = 107.2 secs
npoints curve = 750
>> store(m,'modelequilibrium')
```

During the continuation of the first equilibrium four branching points are detected. These branching points are the initial solutions for heterogeneous equilibria. Repeating the previous steps for the third equilibrium `epidx=3` in both continuation directions yields the eutrophic arc. On this arc no branching point exists. With `store(m,'modelequilibrium')` the results of the continuation process are stored into the results of model `m`.

```
>> contpar='b';epidx=3;[x0 v0 s0 f0 h0]=contep(m,ocEP{epidx},contpar,opt0);
first point found
tangent vector to first point found
elapsed time  = 72.9 secs
npoints curve = 750
>> store(m,'modelequilibrium')
>> contpar='b';epidx=3;[x1 v1 s1 f1 h1]=contep(m,ocEP{epidx},contpar,opt1);
```

```
first point found
tangent vector to first point found
elapsed time  = 76.2 secs
npoints curve = 750
>> store(m,'modelequilibrium')
```

The calculation of the arcs emanating from the branching points are exemplified for the second branching point.

```
>> n=3;m1=changeparametervalue(m,'b',[x0(end,s0(n).index)]);
>> ocEP1=calcep(m1,x0(1:end-1,s0(n).index),0,opt);
>> opt0=setocoptions(opt0,'MATCONT','MaxNumPoints',1500,'MaxStepsize',2e-1,'CheckClosed'
   ,50);
>> epidx=1;[xbp0 vbp0 sbp0 fbp0]=contbp(m1,ocEP1{epidx},s0(n),0.01,opt0);
first point found
tangent vector to first point found
label = BP, x = ( 0.619422 0.619661 0.620389 ... -5.917192 -5.917341 -2.958687 0.721718 )
label = BP, x = ( 0.554176 0.554239 0.554455 ... -6.412585 -6.407783 -3.203096 0.706011 )
label = BP, x = ( 0.398031 0.398863 0.401801 ... -9.309244 -9.141784 -4.542734 0.626785 )

elapsed time  = 249.5 secs
npoints curve = 1500
>> store(m,'modelequilibrium')
```

During the continuation starting from the second branching point, i.e. the bifurcation point stored in the structure `s0` at index `n=3`, further branching points are detected. The branches emanating from these PCSS can be computed in an analogous way. Repeating the previous steps for `n=2,4,5` finally yields all branches of FCSS and PCSS, see Fig. 5a.

Using the solutions of the previous calculations can now be used to find the all FCSS and PCSS equilibria for a specific value of b, e.g. $b = 0.65$

```
>> matRes=matcontresult(m);counter=0;b=0.65;
>> for ii=1:length(matRes), ...
        x0=[matRes{ii}.ContinuationSolution.y;matRes{ii}.ContinuationSolution.userinfo.
   varyparametervalue]; ...
        idx0=cont2idx(x0(end,:),b); ...
        for jj=1:length(idx0); ...
        counter=counter+1;ocEP=calcep(m,x0(1:end-1,idx0(jj)),0,opt); ...
        store(m,ocEP);end,end
```

For $b = 0.65$ there exist 17 equilibria.[6]

We will give a two examples for the calculation of a stable path to an equilibrium that satisfies SPP and that does not satisfy SPP.

B.3 Saddle path calculation

One of the main tasks of `OCMat` is the calculation of a stable path converging to an equilibrium of saddle-type. The computation is done by solving the homotopy problem Eq. (25) or Eq. (29). We start with a problem of the first type.

B.3.1 Stable path when SPP is satisfied

As an example we compute, for the parameter values $b = 0.65$ and $c = 0.5$, the stable path that starts at the states of a defective PCSS (`ocEP{9}`) and converge to the eutrophic FCSS (`ocEP{17}`).[7] First

[6] With `load(m,'%1.2f',[],'b,c')` the model where these equilibria and other numerical results are already stored can be loaded into the MATLAB workspace.

[7] The order refers to the results stored in the file `shallowlakelinecoarse_b_0.65_c_0.50.mat`.

we load the model with the stored data of the equilibria.

```
>> m=stdocmodel('shallowlakelinecoarse');m=changeparametervalue(m,'b,c',[0.65 0.5]);
>> load(m,'%1.2f',1,'b,c');ocEP=equilibrium(m);
```

Next we determine the flat equilibria satisfying SPP and their size of the states.

```
>> idx=find(isflat(m,ocEP{:}) & isspp(m,ocEP{:}))
idx =
     1    17
>> P=state(m,ocEP{1});P(1)
ans =
    0.4530
>> P=state(m,ocEP{17});P(1)
ans =
    1.4370
```

To start the continuation process we change some of the default options and call the initialization function `initocmat_AE_EP`. The truncation time `T` is determined by

$$T = \frac{T_0}{\min_{\xi \in \mathrm{E}^s} |\mathrm{Re}\, \xi|},$$

where T_0 usually is set to 10.

```
>> opt=setocoptions('OCCONTARG','MaxStepWidth',1,'InitStepWidth',5e-1,'CheckAdmissibility',
   'off','SBVPOC','MeshAdaptAbsTol',1e-4,'MeshAdaptRelTol',1e-3,'GENERAL','
   TrivialArcMeshNum',20);
>> eval=real(eig(ocEP{17}));eval(eval>0)=[];T=10/min(abs(eval));
>> sol=initocmat_AE_EP(m,ocEP{17},1:N+1,ocEP{9}.y(1:N+1),opt,'TruncationTime',T);
```

After the initialization process the continuation process is started calling `bvpcont`.

```
>> c=bvpcont('extremal2ep',sol,[],opt);
first solution found
tangent vector to first solution found

 Continuation step No.: 1
 stepwidth: 0.5
 Newton Iterations: 1
 Mesh size: 21
 Continuation parameter: 0.0952864


 Continuation step No.: 15
 stepwidth: 1
 Newton Iterations: 1
 Mesh size: 27
 Continuation parameter: 1.01767

 Target value hit.
 label=HTV
 Continuation parameter=1

elapsed time  = 38.4 secs
>> store(m,'extremal2ep');
>> save(m)
```

Finally the result of the continuation is stored in the model-object `m`, for further use. The `save` command allows to store the entire object, i.e. with the stored results, as a MATLAB data file.

B.3.2 Stable path when SPP is not satisfied

The next example was used for the computation of the second and third homotopy process in Section 4.4.2, cf. Fig. 9c. The parameter values are $b = 0.55$ and $c = 3.0825$. Thus, in a first step we try to find a solution that starts at the states of the flat oligotrophic equilibrium (`ocEP{1}`) and converge to the heterogeneous equilibrium satisfying SPP (`ocEP{7}`). For that reason we repeat the steps of the previous Appendix B.3.1.

```
>> opt=setocoptions(opt,'OCCONTARG','MaxStepWidth',1e1,'InitStepWidth',5e-1,'
   MaxContinuationSteps',30,'SBVPOC','MeshAdaptAbsTol',1e-3,'MeshAdaptRelTol',1e-2);
>> m=changeparametervalue(m,'b,c',[0.55 3.0825]);
>> load(m,'%1.4f',[],'b,c')
The results in the actual model 'm' are overwritten. Proceed? y/(n) : y
>> ocEP=equilibrium(m);
>> eval=real(eig(ocEP{7}));eval(eval>0)=[];T=10/min(abs(eval))
>> sol=initocmat_AE_EP(m,ocEP{7},1:N+1,ocEP{1}.y(1:N+1),opt,'TruncationTime',T);
>> c=bvpcont('extremal2ep',sol,[],opt);
>> store(m,'extremal2ep');ocEx=extremalsolution(m);n=length(ocEx);
```

During the continuation process we encounter that the detected solution does not end "near" the equilibrium, i.e. the used truncation time becomes too short. The reason becomes obvious when we have a look on Fig. 9d. The computed solution path approaches a stable path of the defective PCSS$^-$. Therefore, the time it takes to stay in the vicinity of this equilibrium increases. To overcome this problem we extend the homotopy problem Eq. (25) by letting the truncation time T be a free parameter value and adding a further constraint, that guarantees that the solution $X(\cdot)$ not only ends at the the (linearized) stable manifold, but also satisfies

$$\|X(1) - \hat{X}\| = \varepsilon, \tag{32}$$

with some fixed $\varepsilon > 0$. To start this extended continuation process we use the solution after 30 continuation steps[8] and use the initialization argument `'movinghorizon'`

```
>> sol=initocmat_AE_AE(m,ocEx{n},[1:N+1],ocEP{1}.y(1:N+1),opt,'movinghorizon',1)
>> opt=setocoptions(opt,'OCCONTARG','MaxStepWidth',1e2,'InitStepWidth',5e0,'
   MaxContinuationSteps',70);
>> c=bvpcont('extremal2ep',sol,[],opt);
>> store(m,'extremal2ep');ocEx=extremalsolution(m);n=length(ocEx);
```

Next we compute a stable path that converges to the defective equilibrium PCSS$^-$. The stable manifold of the defective equilibrium (it has defect -1) is of dimension $(N+1)-1$. Taking the initial states $P^d(0)$ of the solution of the last continuation process, in `OCMat` notation `ocEx{n}.y(1:N1,1)+`, there exists κ_1 such that $P_0 = P^d(0) + \kappa_1 v_1$ with $v_1 = (1,\dots,1)^\top \in \mathbb{R}^{N+1}$ is lying in the N-dimensional stable manifold. Thus, we solve the according homotopy problem.

```
>> opt=setocoptions(opt,'OCCONTARG','MaxStepWidth',1e1,'InitStepWidth',1e-1,'SBVPOC','
   MeshAdaptAbsTol',1e-4,'MeshAdaptRelTol',1e-3);
>> V1=ones(N+1,1);eval=real(eig(ocEP{8}));eval(eval>0)=[];T=10/min(abs(eval))
>> sol=initocmat_AE_EP(m,ocEP{8},[1:N+1],ocEx{n}.y(1:N+1,1),opt,'TruncationTime',T,'
   freevector',V1);
>> c=bvpcont('extremal2ep',sol,[],opt);
```

The result of the computations can be plotted using `OCMat` plotting commands.

```
>> clf;xcoord=1;ycoord=2;xvar='spatialnorm';yvar='spatialnorm';
>> plotcont(m,xvar,xcoord,yvar,ycoord,'contfield','ExtremalSolution','Index',[2 4 5]);hold
   on,
```

[8] We therefore set the option `'MaxContinuationSteps',30`.

```
>> plotlimitset(m,xvar,xcoord,yvar,ycoord,'Index',[1 7 8],'Marker','.','MarkerSize',10,'
   showspp',1,'showflat',1);
>> hold off;figure(gcf)
```

B.3.3 Indifference threshold point and manifold

This example presents in detail the computation of the results from Section 4.3.2. First we load the models data, retrieve the equilibria and remove the already stored continuation results.

```
>> m=stdocmodel('shallowlakelinecoarse');m=changeparametervalue(m,'b,c',[0.65 0.5]);
>> load(m,'%1.2f',1,'b,c');ocEP=equilibrium(m);
>> removeresult(m,'Continuation');
```

The solutions that start at the states of the seventh equilibrium, a PCSS^0, and converge to the eutrophic and oligotrophic equilibrium are computed.

```
>> idx=find(~isflat(m,ocEP{:}) & isspp(m,ocEP{:}))
idx =
     4     7
>> opt=setocoptions('OCCONTARG','MaxStepWidth',1e1,'InitStepWidth',5e-1,'CheckAdmissibility
   ','off','SBVPOC','MeshAdaptAbsTol',1e-4,'MeshAdaptRelTol',1e-3,'GENERAL','
   TrivialArcMeshNum',20);
>> eval=real(eig(ocEP{1}));eval(eval>0)=[];T=10/min(abs(eval));
>> sol=initocmat_AE_EP(m,ocEP{1},1:N+1,ocEP{7}.y(1:N+1),opt,'TruncationTime',T);
>> c=bvpcont('extremal2ep',sol,[],opt);
>> store(m,'extremal2ep');ocEx=extremalsolution(m);n=length(ocEx);
>> eval=real(eig(ocEP{17}));eval(eval>0)=[];T=10/min(abs(eval));
>> sol=initocmat_AE_EP(m,ocEP{17},1:N+1,ocEP{7}.y(1:N+1),opt,'TruncationTime',T);
>> c=bvpcont('extremal2ep',sol,[],opt);
>> store(m,'extremal2ep');ocEx=extremalsolution(m);n=length(ocEx);
```

Plotting the objective value (Hamiltonian) shows that the eutrophic solution is the optimal solution. Next the last eutrophic solution is continued (for ten steps) in direction of the oligotrophic equilibrium.

```
>> clf;xcoord=1;ycoord=1;xvar='spatialnorm';yvar='hamiltonian';
>> plotcont(m,xvar,xcoord,yvar,ycoord,'contfield','SliceManifold','Index',[1 2]);figure(gcf
   )
>> opt=setocoptions(opt,'OCCONTARG','InitStepWidth',2.5e0,'MaxContinuationSteps',10);
>> sol=initocmat_AE_AE(m,ocEx{2},1:N+1,ocEP{1}.y(1:N+1),opt);
>> c=bvpcont('extremal2ep',sol,[],opt);
>> store(m,'extremal2ep');ocEx=extremalsolution(m);n=length(ocEx);
```

Comparing the objective value of the solutions for the first and third continuation process yields an (heterogeneous) indifference threshold point. Finally the solutions starting at the indifference threshold point and converging to the FOSS are computed.

```
>> ipt0=findindifferencepoint(m,1,3);
>> opt=setocoptions(opt,'OCCONTARG','InitStepWidth',1e1,'MaxContinuationSteps',inf);
>> eval=real(eig(ocEP{1}));eval(eval>0)=[];T=10/min(abs(eval));
>> sol=initocmat_AE_EP(m,ocEP{1},1:N+1,ipt0,opt,'TruncationTime',T);
>> c=bvpcont('extremal2ep',sol,[],opt);
>> store(m,'extremal2ep');ocEx=extremalsolution(m);n=length(ocEx);
>> sol=initocmat_AE_AE(m,ocEx{2},1:N+1,ipt0,opt);
>> c=bvpcont('extremal2ep',sol,[],opt);
>> store(m,'extremal2ep');ocEx=extremalsolution(m);n=length(ocEx);
```

The analogous computations are done for the second PCSS^0 (`ocEP{4}`), yielding a second (heterogeneous) indifference threshold point.

```
>> opt=setocoptions(opt,'OCCONTARG','MaxStepWidth',1e1,'InitStepWidth',5e-1,'
   MaxContinuationSteps',30);
>> eval=real(eig(ocEP{1}));eval(eval>0)=[];T=10/min(abs(eval));
>> sol=initocmat_AE_EP(m,ocEP{1},1:N+1,ocEP{4}.y(1:N+1),opt,'TruncationTime',T);
>> c=bvpcont('extremal2ep',sol,[],opt);
>> store(m,'extremal2ep');ocEx=extremalsolution(m);n=length(ocEx);
>> opt=setocoptions(opt,'OCCONTARG','MaxContinuationSteps',inf);
>> eval=real(eig(ocEP{17}));eval(eval>0)=[];T=10/min(abs(eval));
>> sol=initocmat_AE_EP(m,ocEP{17},1:N+1,ocEP{4}.y(1:N+1),opt,'TruncationTime',T);
>> c=bvpcont('extremal2ep',sol,[],opt);
>> store(m,'extremal2ep');ocEx=extremalsolution(m);n=length(ocEx);
>> clf;xcoord=1;ycoord=1;xvar='spatialnorm';yvar='hamiltonian';
>> plotcont(m,xvar,xcoord,yvar,ycoord,'contfield','SliceManifold','Index',[6 7]);figure(gcf
   )
>> opt=setocoptions(opt,'OCCONTARG','InitStepWidth',2.5e0,'MaxContinuationSteps',10);
>> sol=initocmat_AE_AE(m,ocEx{7},1:N+1,ocEP{1}.y(1:N+1),opt);
>> c=bvpcont('extremal2ep',sol,[],opt);
>> store(m,'extremal2ep');ocEx=extremalsolution(m);n=length(ocEx);
>> ipt=findindifferencepoint(m,6,8);
>> opt=setocoptions(opt,'OCCONTARG','InitStepWidth',1e1,'MaxContinuationSteps',inf);
>> eval=real(eig(ocEP{1}));eval(eval>0)=[];T=10/min(abs(eval));
>> sol=initocmat_AE_EP(m,ocEP{1},1:N+1,ipt,opt,'TruncationTime',T);
>> c=bvpcont('extremal2ep',sol,[],opt);
>> store(m,'extremal2ep');ocEx=extremalsolution(m);n=length(ocEx);
>> sol=initocmat_AE_AE(m,ocEx{7},1:N+1,ipt,opt);
>> c=bvpcont('extremal2ep',sol,[],opt);
>> store(m,'extremal2ep');ocEx=extremalsolution(m);n=length(ocEx);
```

Finally, we use continuation to find the intermediate indifference threshold points from the transformation of the first to the second indifference threshold point.

```
>> opt=setocoptions(opt,'OCCONTARG','MaxStepWidth',1e1,'InitStepWidth',5e-1,'SBVPOC','
   BCJacobian',0);
>> v=ones(N+1,1);
>> sol=initocmat_AE_IDS(m,ocEx(9:10),v,ipt0,opt);
>> c=bvpcont('indifferencedistribution',sol,[],opt);
>> store(m,'indifferencedistribution');
```

References

E.L. Allgower and K. Georg. *Introduction to Numerical Continuation Methods*. SIAM Classics in Applied Mathematics, Philadelphia, PA, 2003.

W.A. Brock and A. Xepapadeas. Diffusion-induced instability and pattern formation in infinite horizon recursive optimal control. *Journal of Economic Dynamics and Control*, 32(9):2745–2787, 2008.

W.A. Brock, G. Engström, and A. Xepapadeas. Spatial climate-economic models in the design of optimal climate policies across locations. *European Economic Review*, 69(0):78–103, 2014. ISSN 0014-2921. doi: http://dx.doi.org/10.1016/j.euroecorev.2013.02.008.

S.R. Carpenter and W.A. Brock. Spatial complexity, resilience and policy diversity: fishing on lake-rich landscapes. *Ecology and Society*, 9(1), 2004. URL http://www.ecologyandsociety.org/vol9/iss1/art8/.

T. Dohnal, J. Rademacher, H. Uecker, and D. Wetzel. pde2path 2.0, in *ENOC 14*, 2014.

D. Grass. Numerical computation of the optimal vector field in a fishery model. *Journal of Economic Dynamics and Control*, 36(10):1626–1658, 2012. doi: 10.1016/j.jedc.2012.04.006.

D. Grass and H. Uecker. Optimal management and spatial pattern formation in a distributed shallow lake model. Technical report, ORCOS, 2015.

D. Grass, J.P. Caulkins, G. Feichtinger, G. Tragler, and D.A. Behrens. *Optimal Control of Nonlinear Processes: With Applications in Drugs, Corruption, and Terror*. Springer Verlag, Berlin, 2008.

N. Hale. A sixth-order extension to the MATLAB bvp4c Software of J. Kierzenka and L. Shampine. Master's thesis, Imperial College London, 2006.

N. Hale and D.R. Moore. A sixth-order extension to the MATLAB package bvp4c of J. Kierzenka and L. Shampine. Report 08/04, Oxford University Computing Laboratory Numerical Analysis Group, 2008.

O. Heaviside. On operators in physical mathematics. part ii. *Proceedings of the Royal Society of London*, 54(326-330):105–143, 1893. doi: 10.1098/rspl.1893.0059.

J. Kierzenka and L.F. Shampine. A BVP solver based on residual control and the maltab PSE. *ACM Transactions on Mathematical Software (TOMS)*, 27(3):299–316, 2001.

J. Kierzenka and L.F. Shampine. A BVP solver that controls residual and error. *Journal of Numerical Analysis, Industrial and Applied Mathematics*, 3(1–2):27–41, 2008.

T. Kiseleva. *Structural Analysis of Complex Ecological Economic Optimal Control Problems*. PhD thesis, University of Amsterdam, Center for Nonlinear Dynamics in Economics and Finance (CeNDEF), 2011.

T. Kiseleva and F.O.O. Wagener. Bifurcations of optimal vector fields in the shallow lake system. *Journal of Economic Dynamics and Control*, 34(5):825–843, 2010.

Y.A. Kuznetsov. *Elements of Applied Bifurcation Theory*. Springer Verlag, New York, 2nd edition, 1998.

G.M. Lentini. *Boundary value problems over semi-infinite intervals*. PhD thesis, California Institute of Technology, 1978.

M. Lentini and H.B. Keller. Boundary value problems on semi-infinite intervals and their numerical solution. *SIAM Journal on Numerical Analysis*, 17(4):577–604, 1980.

K.G. Mäler, A. Xepapadeas, and A. de Zeeuw. The economics of shallow lakes. *Environmental and Resource Economics*, 26(4):603–624, 2003.

P. Michel. On the transversality condition in infinite horizon optimal problems. *Econometrica*, 50(4): 975–985, 1982.

M. Scheffer. *Ecology of Shallow Lakes*. Kluwer Academic Publishers, Dordrecht, The Netherlands, 1998.

F. Tröltzsch. *Optimale Steuerung partieller Differentialgleichungen*. Vieweg+Teubner, 2009.

H. Uecker. Optimal control and spatial patterns in a semi arid grazing model, 2015.

H. Uecker, D. Wetzel, and J.D.M. Rademacher. pde2path—a Matlab package for continuation and bifurcation in 2D elliptic systems. *Numerical Mathematics: Theory, Methods and Applications*, 7: 58–106, 2014.

F.O.O. Wagener. Skiba points and heteroclinic bifurcations, with applications to the shallow lake system. *Journal of Economic Dynamics and Control*, 27(9):1533–1561, 2003.